Notes for Extrasolar Planets
University of Cambridge, Lent 2022

Aditya Sengupta

June 8, 2022

Contents

Extrasolar Planets **Lent 2022**

Lecture 1: Introduction

Lecturer: Nikku Madhusudhan *21 January* *Aditya Sengupta*

Note: *LaTeX format adapted from template for lecture notes from CS 267, Applications of Parallel Computing, UC Berkeley EECS department.*

We start by defining some overall goals:

1. What surface processes are there?
2. What signals are observable?
3. Do planets have a biosphere?
4. What clues can we get about a planet's formation conditions?
5. Do a star and its planet interact?

Next, we define what we could try and study in atmospheres:

1. T, P, ρ profiles
2. Atmospheric escape
3. Chemical composition
4. Radiative transport
5. Chemical processes
6. Dynamics
7. Clouds and hazes
8. Biosignatures

And in interiors:

1. Composition
2. Structure
3. Formation
4. Energy transport
5. Magnetic fields
6. Geological processes

From this diversity of goals and observables, we can build up a sort of taxonomy of parameters and phenomena in exoplanet characterization, on page 2 of this review paper: `https://arxiv.org/pdf/1402.1169.pdf`.

We'll study atmospheres, then interiors, then formation, and finally astrobiology.

Extrasolar Planets **Lent 2022**

Lecture 2: Inference from transits

Lecturer: Nikku Madhusudhan *24 January* *Aditya Sengupta*

We'll start with some basic observational techniques today.

As a broad overview of what we know of exoplanet detection so far, the first detection was made in 1995. We only knew of the solar system planets back then, so designing a mission to study the planets would inherently mean looking at the solar system planets. The survey strategy for finding new planets would be very heavily based on the specifics of our solar system, which would be kind of difficult because the solar system has either small planets, or planets that are far out, and both of those are difficult to detect. We would need to develop very sensitive detectors, because the theory was similar to how we thought we'd observe faint stars.

Then came 51 Peg b, the first exoplanet detected around a Sun-like star. This was an unexpected discovery, because it had about the mass of Jupiter but it was 100 times closer than Jupiter is to our Sun. Formation theorists couldn't have predicted that close of a separation at the time.

Since then, we've found about 5000 exoplanets, spread across parameter space, and mostly detected using the transit, radial velocity, direct imaging, and gravitational microlensing techniques. The majority of planets we've found are from the transit technique. Most of the exoplanets we've found today have no solar system analogs.

Let's cover the three main techniques: transit, radial velocity, and direct imaging. The easiest and most productive method of detecting exoplanets is the transit technique: if we're able to look at a star-planet system relatively edge-on, when the planet crosses the star, it blocks out some of the light, and there's a dip in brightness. Also, there's a secondary eclipse when the planet crosses the star on the opposite end and additional light from the planet (either in thermal emission or reflected light) gets blocked out.

The magnitude of a transit dip can be calculated. The flux from the star alone, when the planet is not transiting, is proportional to some surface flux F_s times the surface area (proportional to R_s^2; the F_s has a π factor in it), reduced by the distance to the star d

$$F_{\text{out}} = F_s \left(\frac{R_s}{d} \right)^2 \tag{2.1}$$

When you're in transit, you can expect a reduction commensurate with the size of the planet:

$$F_{in} = F_s \left(\frac{R_s^2 - R_p^2}{d^2} \right) \tag{2.2}$$

Therefore, the *relative transit depth* is the size of the dip:

$$\Delta = \frac{F_{out} - F_{in}}{F_{out}} = \frac{R_p^2}{R_s^2}. \tag{2.3}$$

In the case of a Jupiter-like planet around a Sun-like star, $R_s \approx 10R_J$ so we get a 1% transit dip. We want that to be a lot smaller to precisely constrain a transit; for a 10-sigma detection, you therefore want photometric precision to about 0.1%. For Earth around the Sun, $R_s \approx 100R_E$ so we get a transit dip of 0.01%, and so the desired photometric precision comes down to about 10 ppm (parts per million). This seems difficult, but optical engineers are incredible; we've found hundreds of Earth-like planets around Sun-like stars.

The real constraint is needing to find systems where the planets are edge-on. If we look at enough stars, we'll find this, though, and survey missions are designed with this in mind. They look at wide fields of hundreds of thousands of stars and look for periodic dips, and more in-depth follow-up missions can look further at these.

How do we see an atmosphere during a transit? We'll do a full derivation of an atmospheric spectrum in a later lecture, but for now we'll just get a sense of it. Say a planet has an atmosphere of size H on top of its existing radius, meaning we have an effective radius of $R_p' = R_p + H$. This gives us a delta of

$$\Delta = \frac{(R_p + H)^2}{R_s^2} = \frac{R_p^2 + 2R_pH + \cancel{H^2}}{R_s^2}. \tag{2.4}$$

What is H? We can describe the atmosphere to first order using hydrostatic equilibrium, and we can get H in terms of T, μ, g. If the atmosphere is isothermal, we can show $H_{sc} = \frac{kT}{\mu g}$ and $H = NH_{sc}$, where N is some number usually less than 10 parameterising extra processes (mostly the relative abundance of the species causing opacity). The atmosphere adds to the thickness of the planet because we're assuming the atmosphere is opaque, but really the opacity is wavelength-dependent. We can therefore split this up into a function of wavelength, Δ_λ against λ. We can look at the transit depth at different wavelengths λ. This is a continuous function: depending on what we measure, we see different opacities. If the atmosphere were transparent, we'd just see R_p^2/R_s^2, but if there are features adding opacity, those will show up in regions of λ around the expected lines for that species. This is a *transmission spectrum*, meaning it describes the transit depth as it varies with wavelength.

We can compute the size of a spectral feature just by subtracting off the baseline: $\delta = \Delta_\lambda - \Delta_0$, and this equals

$$\delta = \Delta_\lambda - \Delta_0 = \frac{2R_pH_\lambda}{R_s^2} = 2\frac{R_p^2}{R_s^2}\frac{H_\lambda}{R_p} = 2\Delta_0\frac{H_\lambda}{R_p}, \tag{2.5}$$

so if we just measure the optical depth at a wavelength and a baseline, we can get the temperature as it's the only unknown component in H_λ.

This is a zeroth-order analysis, and in future lectures we'll be looking into the complicated versions. For now, let's look at the secondary eclipse. Out of eclipse, we see the reflected light from the day side of the planet, and in eclipse, we see our previous out-of-transit flux:

$$F_{out} = F_s\frac{R_s^2 + R_p^2}{d^2} \tag{2.6}$$

$$F_{in} = F_s\frac{R_s^2}{d^2} \tag{2.7}$$

$$\Delta = \frac{F_{out} - F_{in}}{F_{in}} = \frac{F_p}{F_s}\frac{R_p^2}{R_s^2} \tag{2.8}$$

What are these fluxes? Blackbodies follow the Stefan-Boltzmann law, with proportionality to T^4. This gives you the bolometric flux, integrated over all wavelengths, but here we want to keep the wavelength intact, so we use the Planck function.

$$\Delta = \frac{B_\lambda(T_p)}{B_\lambda(T_s)} \left(\frac{R_p}{R_s}\right)^2 \tag{2.9}$$

where

$$B_\lambda(T) = \frac{2hc^2}{\lambda^5} \frac{1}{e^{hc/\lambda k_B T} - 1} \tag{2.10}$$

In the large-wavelength limit where $\lambda \gg \frac{hc}{k_B T}$, we get

$$B_{\lambda_T} \propto \frac{T}{\lambda^4} \tag{2.11}$$

$$\Delta = \frac{T_p}{T_s} \left(\frac{R_p}{R_s}\right)^2. \tag{2.12}$$

So we get an estimate of planet surface temperature just from the (secondary eclipse) transit at a particular wavelength! Spitzer has been used to do this.

This is also subject to precision constraints: for a hot Jupiter, say $T_p \sim 2000$ K, $\Delta_0 = 0.01, T_s \sim 6000$ K. We get $\Delta \sim 3 \times 10^{-3}$, so we need a higher degree of precision than before.

Extrasolar Planets **Lent 2022**

Lecture 3: Thermal emission and direct imaging

Lecturer: Nikku Madhusudhan *26 January* *Aditya Sengupta*

3.1 Thermal emission spectra

Last time, we worked out the planet-star flux ratio for large λ. What if this assumption doesn't hold? We can qualitatively look at the Planck function against λ for different temperatures, and note that while both curves are falling away from their peak in the large λ limit and therefore that $\frac{F_p}{F_s}$ should be roughly constant in λ in this limit, the Planck function for the star peaks before that for the planet, so after that the star's B_λ is falling and the planet's is rising. This tells us that $\frac{F_p}{F_s}$ is increasing in the low-medium regime.

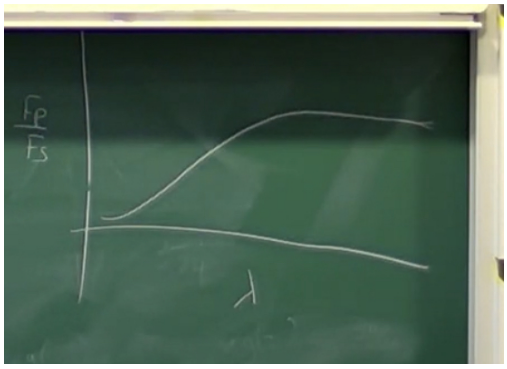

Wien's law tells us that $\lambda_{\max} T$ is constant. For our Sun, $\lambda_{\max} \sim 550$ nm and $T \sim 5800$ K, so we can calculate that constant and can work it out for every other star. We'll work mostly in the infrared in this class. The coolest stars are the late M-dwarfs, which have $T \sim 3000$ K, which gives us a $\lambda_{\max}$ of around 1 μ m. Therefore anything hotter than this will peak at a shorter wavelength, putting most of what we're interested in at the IR and optical ranges. For some other benchmarks: the Earth is about 300 K, so $\lambda_{\max} \sim 10\mu$m, and Jupiter is about 100 K, so $\lambda_{\max} \sim 30\mu$m.

All of this has assumed that stars and planets are blackbodies. For our purposes here, this is a fair assumption for the star, but not so much for the planet. As a first order of complication, let's look at reflection.

$$F_{\text{total,planet}} = F_{\text{thermal,planet}} + cF_{\text{star}}. \tag{3.1}$$

The total planet flux is its thermal emission plus some constant multiple (for the sake of argument; we'll fill this in later) of the stellar flux. This will give us a Planck curve that has two peaks. In practice, it's very hard to detect the reflected starlight component, so this has never been done, but you could theoretically simultaneously fit the star and planet temperatures.

We've looked at two techniques using transits: transmission spectra, and thermal emission/reflection spectra. Now, let's look at some other methods.

3.2 Direct imaging

Transits are somewhat limiting, because they need the solar system to be edge-on, and it favours planets that are very close in. A more obvious strategy would be just to take a picture of the planet. This is harder for two reasons: we don't want the starlight to dwarf the planet, and we need to be able to see the star and the planet as distinct objects, so

1. The planet-star flux contrast has to be high enough
2. The angular separation between the planet and the star has to be resolved.

We can use the same formalism from transits to look at the flux contrast. In the Rayleigh-Jeans limit, we've already seen that $\frac{F_p}{F_s} = \frac{T_p}{T_s}\left(\frac{R_p}{R_s}\right)^2$. For Jupiter, this comes out to around 1.5×10^{-4} and for Earth this is around 5×10^{-6}. However, this limit doesn't actually apply here.

It's especially hard to build good ground-based direct imaging for Earth-like planets at the peak wavelengths (beyond about 5μm it gets difficult), because the Earth itself is a blackbody so its own emission will interfere with observations. From the ground, you need to look in the optical or near-IR, and the required contrast is much higher. For Earth, it becomes around 10^{-9}, and there's no instrument that can do that.

For angular separation, we run into the diffraction limit as a certain point. If we image a star, we get a point image that gets transformed into an Airy disk, whose angular size is $\theta = 1.22\frac{\lambda}{D}$. We can plug in numbers to this ($\lambda = 0.5\mu$m, $D = 10$m) and get the diffraction limit for the best telescopes on Earth right now: $\theta = 0.013$". That's what we can get: what do we need?

For a semimajor axis (mean star-planet separation) a, and a distance d to the system, the angular separation we need to resolve them both is $\theta(") = \frac{a(\text{AU})}{d(\text{pc})}$. Plugging in numbers, we see that we should be able to resolve the Earth-Sun system from 10pc away. However, that's under diffraction-limited conditions, and our seeing from Earth is a lot worse than that. The best we can get is about 0.2", even with adaptive optics. If we go to space, it gets much easier, but we're then limited by the maximum diameter we can send.

On top of this, the best planet-star flux contrast we can currently achieve is about 10^{-5}. It seems like direct imaging just doesn't work for the scales we're interested in. So how are we doing it?

If you catch planets early in their formation, they're extremely hot, which makes the contrast better while not making the angular resolution worse. This lets us get $\frac{F_p}{F_s} \sim 10^{-4}$ in the near-IR. The solution is to look at young giant planets at large separations.

Extrasolar Planets **Lent 2022**

Lecture 4: How to look at exoplanet spectra

Lecturer: Nikku Madhusudhan *28 January* *Aditya Sengupta*

4.1 Observations of spectra

Last time, we saw how the transit depth and occultation depth related to the planet and star temperatures and radii. We saw how we could derive an atmospheric spectrum, to zeroth order, with these estimates. To start today, we'll look at how the radial velocity method works.

A star-planet system orbits their common center of mass, meaning the star has a small rotation due to the gravitational effect of the planet. This results in a Doppler shift from the observer perspective, which we can observe to infer a minimum mass of the planet. You get a radial velocity curve as a function of time, which is ideally a sine wave. The period is the planet's period, and the amplitude is $\frac{M_p \sin i}{M_s^{2/3}}$. This was the technique they used to detect the first exoplanet around a Sun-like star, and radial velocity observations are useful for follow-ups of transit surveys so you can constrain masses.

We're in a golden age of exoplanet science: there's revolutions in detection (especially of small planets around nearby stars), and characterization. The main reason for this is survey missions: NGTS, TESS, CHEOPS, and in a few years PLATO. In characterization, we have JWST, in a few years ARIEL, and ELT-class telescopes.

The big question in the field is: how diverse are exoplanetary atmospheres? To do this, it's useful to look at the detection biases of the methods we've seen. For transits in particular, there's a bias based on $(R_p/R_s)^2$; to look at small planets, we want to look at small stars. It also helps to look at nearby planets, so that the flux is high.

We characterise the atmospheric spectrum of a transiting planet, to zeroth order, by looking for absorption peaks at characteristic wavelengths of size δ:

$$\delta = \Delta - \Delta_0 = \frac{2R_p H}{R_s^2} = \Delta_0 \frac{2H}{R_p} \tag{4.1}$$

Ground-based and space-based transmission spectra have achieved very good SNRs in the past decade, under good conditions.

Also: fun sightings of familiar names! Marois and Konopacky.

So how about characterization with RV? If we look in the infrared with a high-resolution spectrograph, we see that the planet's thermal emission spectrum is Doppler-shifted just like the star's is! We see the thermal emission of the planet if the planet-star flux contrast is high enough, and so close to transit and secondary eclipse especially, you can look at the spectrum (only at the part that's changing, so that you can remove the Earth's and the star's influence) and monitor the molecular lines going back and forth with the Doppler shift. The models have to be incredibly high fidelity: lines are very thin and closely spaced.

With infrared observations, you probe quite deep in the planet atmosphere, and less so with optical and even less with UV. This means based on the wavelength you're probing, you can understand a different part

of the atmosphere. We make chemical detections in each region of the atmosphere, and consider what they tell us about the processes going on; we say these molecules are *tracers* of the processes. There's a lot of atmospheric processes: radiative transfer, atmospheric escape, photochemistry, thermal inversions, clouds and hazes, vertical mixing, atmospheric circulation, and at the bottom-most level chemical equilibrium.

4.2 Radiative transfer

Our only point of observation in exoplanet atmospheres is a spectrum (transmission or emission). Our fundamental question is: what do we observe as a function of the planet's properties? Let's define a few quantities that will help us derive those observables.

Take an area element $\mathrm{d}A$ with a normal to it in the $\hat{z}$ direction, and a beam coming out of it into a solid angle $\mathrm{d}\omega$ in a direction $\hat{n}$. The *specific intensity* I_ν is defined as the amount of energy per unit frequency interval (or wavelength interval) passing through a unit area normal to the beam (this is where we get the $\mathrm{d}A\cos\theta$ term) into a unit solid angle in unit time.

$$\mathrm{d}E = I_\nu(\vec{r},\vec{n})\mathrm{d}\nu\mathrm{d}t\mathrm{d}\omega\mathrm{d}A\cos\theta. \tag{4.2}$$

This has an interesting property: that of *invariance*. Take a source and a detector, with different angles and area elements (resp. $\theta, \mathrm{d}A$ and $\theta', \mathrm{d}A'$) and look at the energy at both. At the source, this is $\mathrm{d}E = I_\nu \mathrm{d}\nu\mathrm{d}t\frac{\mathrm{d}A'\cos\theta'}{d^2}\mathrm{d}A\cos\theta$, and at the detector, this is $\mathrm{d}E' = I'_\nu\mathrm{d}\nu\mathrm{d}t\frac{\mathrm{d}A\cos\theta}{d^2}\mathrm{d}A'\cos\theta'$. In both, we've considered $\mathrm{d}\omega = \frac{\mathrm{d}A'\cos\theta'}{d^2}$ by considering the solid angle subtended by the detector (and flip the primes for the solid angle subtended by the source) and looking at the distance and projected area of the other surface that subtends that angle. By conservation of energy, $\mathrm{d}E = \mathrm{d}E' \implies I_\nu = I'_\nu$, assuming there is no source or sink in between. The star or the atmosphere can be this source or sink.

Extrasolar Planets **Lent 2022**

Lecture 5: Flux, atmospheres

Lecturer: Nikku Madhusudhan *31 January* *Aditya Sengupta*

5.1 Flux continued

Last lecture, we started looking at specific intensity. We defined it as the energy in a beam going away from a source, the geometry of which induces several unit dependences:

$$\mathrm{d}E = I_\nu \mathrm{d}\omega \mathrm{d}A \cos\theta \mathrm{d}\nu \mathrm{d}t. \tag{5.1}$$

The energy emitted in a source-detector setup is

$$\mathrm{d}E = I_\nu \mathrm{d}\omega \mathrm{d}A \cos\theta \mathrm{d}\nu \mathrm{d}t = I_\nu \mathrm{d}A \cos\theta \mathrm{d}\nu \mathrm{d}t \frac{\mathrm{d}A' \cos\theta'}{d^2}, \tag{5.2}$$

since we can calculate the solid angle for the source-detector setup as $\mathrm{d}\omega = \frac{\mathrm{d}A' cos\theta'}{d^2}$, and similarly the other way to be $\mathrm{d}\omega' = \frac{\mathrm{d}A cos\theta}{d^2}$. Applying conservation of energy $\mathrm{d}E = \mathrm{d}E'$, we get $I_\nu = I'_\nu$.

I_ν carries units of ergs/cm^2/Hz/s/sr. To get the flux (counts per unit area per time per frequency) on a detector, we integrate out the sr part. In full generality, if I want the flux in a direction, we give the specific intensity a direction component (the direction of propagation), and we integrate over the solid angle of the beam.

$$\vec{F_\nu} = \int_\Omega I_\nu \vec{n} \mathrm{d}\omega. \tag{5.3}$$

Place the observer along the $\hat{z}$ direction. We can get the (scalar) flux at the source in the direction of the observer by

$$F_{\nu,\mathrm{s}} = \int_\Omega \hat{n} \cdot \hat{z} \mathrm{d}\omega = \int_\Omega I_\nu \cos\theta \mathrm{d}\omega. \tag{5.4}$$

We know that $\mathrm{d}\omega = \sin\theta \mathrm{d}\theta \mathrm{d}\phi$, so we can compute this:

$$F_{\nu,\mathrm{s}} = \int_\Omega I_\nu \cos\theta \sin\theta \mathrm{d}\theta \mathrm{d}\phi. \tag{5.5}$$

Now, we need to parameterise Ω. We'll assume we have plane-parallel geometry, where the source plane is flat: this gives us θ from 0 to $\frac{\pi}{2}$, and ϕ from 0 to 2π.

$$F_{\nu,\mathrm{s}} = \int_0^{2\pi} \int_0^{\frac{\pi}{2}} I_\nu \cos\theta \sin\theta \mathrm{d}\theta \mathrm{d}\phi. \tag{5.6}$$

For now, we'll assume that we have isotropic I_ν, i.e. it's a constant with respect to θ, ϕ, so

$$F_{\nu,\mathrm{s}} = \pi I_\nu. \tag{5.7}$$

This is sometimes referred to as the astrophysical flux.

Let's find the flux at the detector now. Consider a uniformly isotropically emitting sphere. We look at it from a distance d. As before, we look at

$$F_{\mathrm{obs}} = \int_\Omega I \mathrm{d}\omega. \tag{5.8}$$

Assume that $d \gg R$, so rays are parallel. We take an area element at a radius $x < R$. The observer sees a disk, which is a circle of radius x and an infinitesimal thickness $\mathrm{d}x$, so the contribution to ω from this annulus is

$$\mathrm{d}\omega = \frac{2\pi x \mathrm{d}x}{d^2}. \tag{5.9}$$

We can rewrite $x = R\sin\theta$ so that we're able to do the solid angle integral.

$$\mathrm{d}\omega = \frac{2\pi R^2 \sin\theta\cos\theta \mathrm{d}\theta}{d^2}. \tag{5.10}$$

This gives us

$$F_{\nu,\mathrm{obs}} = \int_\Omega I_\nu \mathrm{d}\omega = \int I_\nu \frac{2\pi R^2}{d^2} \sin\theta\cos\theta \mathrm{d}\theta \tag{5.11}$$

The $\cos\theta$ term comes back here: the difference between this one and the last one just comes down to *when* you do the projection into the plane the observer can see, but you have to do it regardless.

We run through a similar set of computations as we did last time:

$$F_{\nu,\mathrm{obs}} = 2\pi I_\nu \frac{R^2}{d^2} \int_0^{\frac{\pi}{2}} \sin\theta\cos\theta \mathrm{d}\theta = \pi I_\nu \frac{R^2}{d^2}. \tag{5.12}$$

Therefore $F_{\nu,\mathrm{obs}} = F_{\nu,s}\frac{R^2}{d^2}$.

Slight detour: if you assume a blackbody, the flux at the source in the direction of the observer is $F_{\nu,\mathrm{s}} = \pi B_\nu$, and at the observer it's $F_{\nu,\mathrm{obs}} = \pi B_\nu \frac{R^2}{d^2}$. If we want the bolometric flux, we integrate this over frequency.

$$F_\mathrm{s} = \int_0^\infty F_{\nu,\mathrm{s}} \mathrm{d}\nu = \pi \int_0^\infty B_\nu \mathrm{d}\nu. \tag{5.13}$$

If you do this integral, you'll get σT^4, which is the Stefan-Boltzmann law.

5.2 Atmospheres

All of these calculations are for the case with nothing in between. If thre's some medium (an atmosphere, as the example we care the most about) how does this change?

We'll start by defining a simple version of the radiative transfer equation, in one dimension. Take a medium with cross-section $\mathrm{d}A$ and thickness $\mathrm{d}s$. We'll send a beam through it, and see what happens when it comes out as a function of those properties.

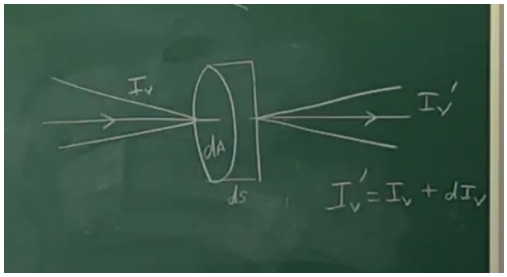

We expect $I'_\nu = I_\nu + \mathrm{d}I_\nu$, where $\mathrm{d}I_\nu$ might be positive or negative.

The first case we'll look at for what could happen is absorption, which we characterise using the absorption coefficient κ_ν. This is the absorption cross-section per unit mass, and has units of cm^2/g. The energy is

$$\mathrm{d}E_\nu = I_\nu \mathrm{d}\omega \mathrm{d}\nu \mathrm{d}t \kappa_\nu \mathrm{d}m. \tag{5.14}$$

We'll say the density ρ is known, so we can substitute $\mathrm{d}m = \rho \mathrm{d}A\mathrm{d}s$.

$$\mathrm{d}E_{\nu,\mathrm{abs}} = I_\nu \kappa_\nu \rho \mathrm{d}A\mathrm{d}s\mathrm{d}\omega\mathrm{d}\nu\mathrm{d}t. \tag{5.15}$$

Another thing that could happen is scattering, which means some of the incoming radiation is scattered away from the outgoing beam: it's going somewhere that is not the direction of the outgoing beam. This is characterised using the scattering coefficient σ_ν.

$$\mathrm{d}E_{\nu,\mathrm{sc}} = I_\nu \sigma_\nu \rho \mathrm{d}A\mathrm{d}s\mathrm{d}\omega\mathrm{d}\nu\mathrm{d}t. \tag{5.16}$$

The third thing is emission. This shouldn't be dependent on the incoming beam (it can, but not in this simple setup), and is instead just a property of the medium. This is characterised using the emissivity j_ν.

$$\mathrm{d}E_{\nu,\mathrm{em}} = j_\nu \rho \mathrm{d}A \mathrm{d}s \mathrm{d}\omega \mathrm{d}\nu \mathrm{d}t. \tag{5.17}$$

We've got all the terms, now we'll just look at the energy balance. The net energy gain is

$$\mathrm{d}E_\nu = \mathrm{d}I_\nu \mathrm{d}A \mathrm{d}\omega \mathrm{d}\nu \mathrm{d}t \tag{5.18}$$

but it's also equal to the gain terms minus the loss terms,

$$\mathrm{d}E_\nu = \mathrm{d}E_{\nu,\mathrm{em}} - (\mathrm{d}E_{\nu,\mathrm{abs}} + \mathrm{d}E_{\nu,\mathrm{sc}}). \tag{5.19}$$

Plug these things in, and we get

$$\mathrm{d}I_\nu = j\rho \mathrm{d}s + (\kappa_\nu + \sigma_\nu)\rho \mathrm{d}s I_\nu \tag{5.20}$$

$$\frac{1}{\rho}\frac{\mathrm{d}I_\nu}{\mathrm{d}s} = j_\nu - k_\nu I_\nu, \tag{5.21}$$

where we have $k_\nu = \kappa_\nu + \sigma_\nu$. This is the *radiative transfer equation*.

Attenuation is determined mostly by the $\mathrm{d}s$ term: it matters more how far a beam travels.

Extrasolar Planets **Lent 2022**

Lecture 6: Radiative transfer applied to atmospheres

Lecturer: Nikku Madhusudhan *2 February* *Aditya Sengupta*

We started last time with specific intensity I_ν which had units of ergs/cm^2/Hz/s/sr. To see the flux, we derived the simple formula $F_s = \pi I_\nu$. At the observer, we found that $F_{\nu,\text{obs}} = F_s \frac{R^2}{d^2}$. We saw that for a blackbody, $I_\nu = B_\nu$ and the other quantities follow; in particular, $F_{\text{tot}} = \int_0^\infty \pi B_\nu \mathrm{d}\nu = \sigma T^4$.

We derived an expression for energy attenuation when passing through a medium with cross-section area $\mathrm{d}A$ and thickness $\mathrm{d}s$. We also know by definitions that $\mathrm{d}E_\nu = \mathrm{d}I_\nu \mathrm{d}\omega \mathrm{d}\nu \mathrm{d}t \mathrm{d}A$. We can also compute the net energy gain in terms of the absorption/emission/scattering coefficients, which gives us the radiative transfer equation when we set those two equal:

$$\mathrm{d}I_\nu \mathrm{d}\omega \mathrm{d}\nu \mathrm{d}t \mathrm{d}A = j_\nu \rho \mathrm{d}A \mathrm{d}s \mathrm{d}\omega \mathrm{d}\nu \mathrm{d}t - \underbrace{(\kappa_\nu + \sigma_\nu)}_{k_\nu} \rho \mathrm{d}A \mathrm{d}s I_\nu \mathrm{d}\omega \mathrm{d}\nu \mathrm{d}t \tag{6.1}$$

$$\frac{1}{\rho}\frac{\mathrm{d}I_\nu}{\mathrm{d}s} = j_\nu - k_\nu I_\nu. \tag{6.2}$$

We often refer to k_ν as the *extinction coefficient*. The ratio $\frac{j_\nu}{k_\nu}$ (emission over extinction) is often referred to as the *source function* S_ν. We can rewrite the radiative transfer equation as

$$\frac{\mathrm{d}I_\nu}{k_\nu \rho \mathrm{d}s} = S_\nu - I_\nu. \tag{6.3}$$

This is a first-order differential equation, and it can have varying levels of complexity depending on the physics we consider. It's often useful to split $j_\nu = j_\nu^t + j_\nu^s$, for thermal and scattering (into the direction of the beam) terms.

To specify our emission term, we'll use a physical principle called local thermodynamic equilibrium (LTE), in which we assume the material is in a cavity of uniform temperature with perfectly absorbing and emitting walls (the same idea as a blackbody), and the material is in equilibrium with the radiation field. This assumption, balancing thermal emission with absorption, gives us $j_\nu^t = \kappa_\nu B_\nu(T)$, the *Kirchhoff-Planck law*. This is an idealized condition, but it's a good approximation deep in the atmosphere, and it allows for an analytical solution to the radiative transfer equation.

Next, we'll look at the scattering term. We consider a simplistic case where scattering is isotropic (no preferential angle for scattering) and coherent (the scattering does not change the frequency of a photon).

$$j_\nu^s = \sigma_\nu J_\nu, \tag{6.4}$$

where J_ν is the mean intensity $\frac{1}{4\pi}\int_\Omega I_\nu \mathrm{d}\omega$. This gives us

$$S_\nu = \frac{j_\nu}{k_\nu} = \frac{\kappa_\nu B_\nu}{\kappa_\nu + \sigma_\nu} + \frac{\sigma_\nu J_\nu}{\kappa_\nu + \sigma_\nu} \tag{6.5}$$

For the special case where we have LTE and no scattering, we get $\sigma_\nu = 0$ and so $S_\nu = B_\nu$. So we have a simplistic representation of the source function.

Let's start applying this to atmospheres! We'll do transmission geometry first. Let's assume the source function is weak compared to the incident radiation: $S_\nu \ll I_\nu$.

$$\frac{1}{k_\nu \rho}\frac{\mathrm{d}I_\nu}{\mathrm{d}s} = -I_\nu \tag{6.6}$$

This can be solved by separation of variables (where we replace $\mathrm{d}s = \frac{\mathrm{d}z}{\cos\theta}$ and for convenience we write $\mu = \cos\theta$):

$$\frac{\mathrm{d}I_\nu}{I_\nu} = -\kappa_\nu \rho \mathrm{d}s = -\frac{\kappa\rho \mathrm{d}z}{\mu}. \tag{6.7}$$

We combine this numerator into the *optical depth*,

$$\frac{\mathrm{d}I_\nu}{I_\nu} = -\frac{\mathrm{d}\tau_\nu}{\mu} \tag{6.8}$$

$$I_\nu = I_{\nu,0} e^{-\tau_\nu/\mu} \tag{6.9}$$

This is similar to the Beer-Lambert law in chemistry.

Let's go back to our planet in front of a star. Going back to the geometry of an annulus, we write $\mathrm{d}\omega = \frac{2\pi x \mathrm{d}x}{d^2}$, and this gives us

$$F_{out} = \int_\Omega I_\nu \mathrm{d}\omega = \int_0^R \frac{2\pi x \mathrm{d}x}{d^2} I_\nu = \pi I_\nu \frac{R^2}{d^2} \tag{6.10}$$

Applied to just a star (for out of transit),

$$F_{out} = \pi I_{\nu,s} \frac{R_s^2}{d^2}. \tag{6.11}$$

And applied to a star-planet system (in transit),

$$F_\nu = \frac{2\pi}{d^2}\left[\int_0^{R_p} I_{p,\nu} x \mathrm{d}x + \int_{R_p}^{R_s} I_{s,\nu} x \mathrm{d}x\right]. \tag{6.12}$$

With the simplifying assumption that $I_{p,\nu} \ll I_{s,\nu}$, the effect is basically just to block out a portion of the light:

$$F_\nu = \pi I_s (R_s^2 - R_p^2)/d^2. \tag{6.13}$$

However, this isn't the only factor – let's apply this same method to a star-planet-atmosphere system:

$$F_\nu = \frac{2\pi}{d^2}\left[\int_0^{R_p} I_{p,\nu} x \mathrm{d}x + \int_{R_p}^{R_p+H} I^a_{p,\nu} x \mathrm{d}x + \int_{R_p+H}^{R_s} I_{s,\nu} x \mathrm{d}x\right] \tag{6.14}$$

We say the first term goes away, and assuming a constant optical depth for simplicity ($I^a_{p,\nu} = I_{s,\nu} e^{-\tau_\nu}$), we substitute in the exponential dependence on optical depth we got before,

$$F_\nu = \frac{\pi I_{s,\nu}}{d^2}\left[2R_p H e^{-\tau_\nu} + R_s^2 - R_p^2 - 2R_p H\right] \tag{6.15}$$

$$F_\nu = \frac{\pi I_{s,\nu}}{d^2}\left[R_s^2 - R_p^2 - 2R_p H(1 - e^{-\tau_\nu}).\right] \tag{6.16}$$

Extrasolar Planets **Lent 2022**

Lecture 7: The origin of spectral features

Lecturer: Nikku Madhusudhan *4 February* *Aditya Sengupta*

Last time, we derived the radiative transfer equation in terms of a source function,

$$\frac{1}{k_\nu \rho}\frac{\mathrm{d}I_\nu}{\mathrm{d}s} = S_\nu - I_\nu, \tag{7.1}$$

where we replaced $\mathrm{d}s$ by $\frac{\mathrm{d}z}{\mu}$, and looked specifically at the case with a negligible source function. We further derived a first-order way to estimate the height of the atmosphere by computing flux in terms of specific intensity and integrating separately over the planet (negligible), the atmosphere, and the unobscured portion of the star.

$$\begin{aligned} F_\nu &= \int_{R_p}^{R_p+H} I^s_{\nu,p}\frac{2\pi x \mathrm{d}x}{d^2} + \int_{R_p+H}^{R_s} I_{\nu,s}\frac{2\pi x \mathrm{d}x}{d^2} \\ &= \frac{2\pi}{d^2} I_{s,\nu} e^{-\tau_\nu}\left[\frac{x^2}{2}\right]_{R_p}^{R_p+H} + \frac{2\pi}{d^2} I_{\nu,s}\left[\frac{x^2}{2}\right]_{R_p+H}^{R_s} \\ &= \frac{\pi I_{\nu,s}}{d^2}\left[R_s^2 - R_p^2 - 2R_pH(1-e^{-\tau_\nu})\right] \end{aligned} \tag{7.2}$$

Let's find the transit depth in this formulation:

$$\Delta = \frac{F_{\nu,\text{out}} - F_{\nu,\text{in}}}{F_{\nu,\text{out}}} = \frac{R_p^2 + 2R_pH(1-e^{-\tau_\nu})}{R_s^2}. \tag{7.3}$$

Looking at some limiting cases, we find that for no atmosphere we get the zeroth-order transit depth of R_p^2/R_s^2, and for an optically thick atmosphere, we get $\tau_\nu \to \infty$ implying $\Delta = \frac{R_p^2+2R_pH}{R_s^2}$. For an optically thin atmosphere, we can Taylor expand the exponential term and just get linear dependence on τ_ν, so we get $\Delta = \frac{R_p^2+2R_pH\tau_\nu}{R_s^2}$.

7.1 Emission spectrum

Let's start again with the radiative transfer equation, and apply it to a secondary eclipse.

$$\frac{\mu}{k_\nu \rho}\frac{\mathrm{d}I_\nu}{\mathrm{d}z} = S_\nu - I_\nu. \tag{7.4}$$

Consider only thermal emission, and say the atmosphere is in LTE with no scattering. Therefore $S_\nu = B_\nu$, and $k_\nu = \kappa_\nu$. We can therefore write

$$\mu \frac{\mathrm{d}I_\nu}{\mathrm{d}\tau_\nu} = I_\nu - B_\nu. \tag{7.5}$$

B_ν is changing with respect to τ_ν, so separation won't work. We'll use an integrating factor: multiply by $e^{-\tau/\mu}$.

$$\mu e^{-\tau_\nu/\mu} \frac{\mathrm{d}I_\nu}{\mathrm{d}\tau_\nu} = I_\nu e^{-\tau_\nu/\mu} - B_\nu e^{-\tau_\nu/\mu} \tag{7.6}$$

$$\frac{\mathrm{d}\left(I_\nu e^{-\tau_\nu/\mu}\right)}{\mathrm{d}\tau_\nu} = -\frac{B_\nu}{\mu} e^{-\tau_\nu/\mu}. \tag{7.7}$$

Then, we integrate both sides from τ_1 (at $z' = 0$) to τ_2 (at $z' = z$).

$$\int_{\tau_1}^{\tau_2} \mathrm{d}\left(I_\nu e^{-\tau_\nu/\mu}\right) = -\int_{\tau_1}^{\tau_2} \frac{B_\nu}{\mu} e^{-\tau_\nu/\mu} \mathrm{d}\tau_\nu \tag{7.8}$$

$$I_\nu(\tau_2) e^{-\tau_2/\mu} - I_\nu(\tau_1) e^{-\tau_1/\mu} = -\frac{1}{\mu} \int_{\tau_1}^{\tau_2} B_\nu e^{-\tau_\nu/\mu} \mathrm{d}\tau_\nu \tag{7.9}$$

$$I_\nu(z) = I_\nu(0) e^{(\tau_2 - \tau_1)/\mu} - e^{\tau_2/\mu} \int_{\tau_1}^{\tau_2} B_\nu e^{-\tau_\nu/\mu} \mathrm{d}\tau_\nu. \tag{7.10}$$

We can further let $\tau_1 \to \infty, \tau_2 \to 0$ and consider the semi-infinite atmosphere. The first term vanishes because $e^{-\infty} \to 0$.

Let's look at an isothermal atmosphere, where B_ν is constant.

$$I_\nu = \frac{1}{\mu} \int_0^\infty B_\nu e^{-\tau_\nu/H} \mathrm{d}\tau_\nu = -B_\nu \, e^{-\tau_\nu/\mu} \Big|_0^\infty = B_\nu. \tag{7.11}$$

This is a reassuring result: an isothermal atmosphere radiates at the temperature at which we would expect it to radiate.

It's difficult to do this analytically without a constant B_ν, but we can look at just one layer. Let's look at a thin layer in which T remains constant but τ varies.

$$I_\nu(z) = I_\nu(0) e^{\tau_2 - \tau_1} - e^{\tau_2} B_\nu (e^{-\tau_1} - e^{-\tau_2}) \tag{7.12}$$

$$I_\nu(z) = I_\nu(0) e^{\tau_2 - \tau_1} + B_\nu (1 - e^{\tau_2 - \tau_1}). \tag{7.13}$$

Further, let's assume $\tau := \tau_1 - \tau_2 \ll 1$. We can Taylor expand both of the exponential terms,

$$I_\nu(z) = I_\nu(0) + \tau(B - I_\nu(0)). \tag{7.14}$$

When B_ν is greater than $I_\nu(0)$, then $I_\nu(z) > I_\nu(0)$, so we're adding intensity to the beam, and we have an emission feature. When B_ν is less than $I_\nu(0)$, then $I_\nu(z) < I_\nu(0)$, so we're subtracting intensity from the beam, and we have an absorption feature. This is the origin of spectral features in an atmosphere!

Extrasolar Planets **Lent 2022**

Lecture 8: Atmosphere theory

Lecturer: Nikku Madhusudhan *7 February* *Aditya Sengupta*

Previously, we were looking at emission geometry through an atmosphere of varying optical depth, and we derived this intensity expression:

$$I_\nu(z) = I_\nu(0)e^{(\tau_2-\tau_1)/\mu} + e^{\tau_2/\mu}\int_{\tau_2}^{\tau_1}\frac{B_\nu e^{-\tau_\nu/\mu}}{\mu}\mathrm{d}\tau_\nu. \tag{8.1}$$

We assumed a semi-infinite isothermal atmosphere, giving us $\tau_2 = 0, \tau_1 = \infty$, and B_ν constant. This gave us $I_\nu(z) = B_\nu$

We further showed how spectral features originate. Consider a thin atmospheric layer such that there's an incident intensity I_0 and outgoing intensity $I(z)$, with a small change in optical depth: $\tau_1 - \tau_2 := \tau \ll 1$, and such that the temperature in the thin layer is constant. We'll also assume normal incidence, so $\mu = 1$. Applying the above formula here gave us

$$I_\nu(z) = I_{\nu,0}e^{-\tau_\nu} + B_\nu e^{\tau_2}(e^{-\tau_2} - e^{-\tau_1}) \tag{8.2}$$

$$= I_{\nu,0}e^{-\tau_\nu} + B_\nu(1 - e^{-\tau_\nu}), \tag{8.3}$$

and since $\tau_\nu \ll 1$, we can Taylor expand to get

$$I_\nu(z) = I_\nu(0) + \tau(B_\nu - I_\nu(0)). \tag{8.4}$$

If $B_\nu < I_{\nu,0}$, we get $I_\nu(z) < I_{\nu,0}$, so less intensity comes out than went in, so we get an absorption feature. If $B_\nu > I_{\nu,0}$, we get $I_\nu(z) > I_{\nu,0}$, so more intensity comes out than went in, so we get an emission feature.

These work only when $\tau_\nu > 0$. To see a spectral feature, you need to ensure both that the source function is sufficiently large and that there is sufficient opacity.

We've seen how spectra originate from underlying atmospheric properties. Given the atmosphere, we know how to study the radiation. Next, let's look at how the atmospheric properties themselves have been influenced by the radiation.

The dominant mechanisms of energy transfer in atmospheres are convection and radiation (conduction isn't as good in gases). We'll primarily look at energy transfer via radiation. We should have a condition of radiative equilibrium: the total energy entering the system should be equal to the total energy leaving. Dropping factors like volume and time that are the same for both,

$$\mathrm{d}E_{\text{loss}} = \int_\nu\int_\Omega k_\nu I_\nu \mathrm{d}\omega\mathrm{d}\nu \tag{8.5}$$

$$\mathrm{d}E_{\text{gain}} = \int_\nu\int_\Omega j_\nu \mathrm{d}\omega\mathrm{d}\nu = \int_\nu\int_\Omega k_\nu S_\nu \mathrm{d}\omega\mathrm{d}\nu. \tag{8.6}$$

We'll further assume an isotropic source function, so we can factor out the solid angle integral and get

$$\mathrm{d}E_{\text{gain}} = 4\pi \int_\nu k_\nu S_\nu \mathrm{d}\nu \tag{8.7}$$

We'll further use the mean intensity $J_\nu = \frac{1}{4\pi}\int_\Omega I_\nu \mathrm{d}\omega$.

Putting these together, we get

$$\mathrm{d}E_{\text{loss}} = \mathrm{d}E_{\text{gain}} \tag{8.8}$$

$$4\pi \int_0^\infty k_\nu J_\nu \mathrm{d}\nu = 4\pi \int_0^\infty k_\nu S_\nu \mathrm{d}\nu \tag{8.9}$$

$$\int_0^\infty k_\nu (J_\nu - S_\nu)\mathrm{d}\nu = 0. \tag{8.10}$$

For LTE with coherent scattering, our source function is $\frac{\kappa_\nu B_\nu + \sigma_\nu J_\nu}{k_\nu}$, which we can plug back in to get

$$\int_0^\infty \kappa_\nu (J_\nu - B_\nu)\mathrm{d}\nu = 0. \tag{8.11}$$

These are powerful expressions for radiative equilibrium. This is the first time we're seeing temperature show up as a factor that determines some part of the radiation field: J_ν and B_ν are complementary, so varying temperature varies B_ν varies J_ν.

Now, let's look at the temperature structure of an atmosphere. Consider the case of an isolated atmosphere heated from below, and look at plane-parallel geometry for a grey atmosphere.

As always, we start with the radiative transfer equation:

$$\mu \frac{\mathrm{d}I_\nu}{\mathrm{d}\tau_\nu} = I_\nu - B_\nu. \tag{8.12}$$

We'll take moments of this equation over μ. To do this, we'll first look at moments of I_ν.

First, some scratch work: $\mathrm{d}\omega = \sin\theta \mathrm{d}\theta \mathrm{d}\phi$, and $\mu = \cos\theta$, so $\mathrm{d}\omega = -\mathrm{d}\mu\mathrm{d}\phi$. This lets us conveniently compute the zeroth moment in μ of I_ν:

$$J_\nu = \frac{1}{4\pi}\int_\Omega I_\nu \mathrm{d}\omega = \frac{1}{4\pi}\int_0^{2\pi}\int_{-1}^1 I_\nu \mathrm{d}\mu\mathrm{d}\theta \tag{8.13}$$

$$J_\nu = \frac{1}{2}\int_{-1}^1 I_\nu \mathrm{d}\mu. \tag{8.14}$$

The first moment H_ν is called the *Eddington flux*, and it's related to flux by $F_\nu = 4\pi H_\nu$:

$$H_\nu = \frac{1}{2}\int_{-1}^{1} \mu I_\nu \mathrm{d}\mu, \tag{8.15}$$

and the second moment is just called the K-integral, and it's to do with radiation pressure but we just care that it's an expression we can use for now,

$$K_\nu = \frac{1}{2}\int_{-1}^{1} \mu^2 I_\nu \mathrm{d}\mu. \tag{8.16}$$

With this, we take the zeroth moment of RTE:

$$\frac{1}{2}\int_{-1}^{1} \mu \frac{\mathrm{d}I_\nu}{\mathrm{d}\tau_\nu}\mathrm{d}\mu = \frac{1}{2}\int_{-1}^{1} (I_\nu - B_\nu)\mathrm{d}\mu. \tag{8.17}$$

Simplifying, this gives us

$$\frac{\mathrm{d}}{\mathrm{d}\tau_\nu} H_\nu = J_\nu - B_\nu \tag{8.18}$$

or

$$\frac{1}{\rho}\frac{\mathrm{d}H_\nu}{\mathrm{d}z} = -k_\nu(J_\nu - B_\nu), \tag{8.19}$$

and we can integrate this over ν to get

$$\frac{1}{\rho}\frac{\mathrm{d}}{\mathrm{d}z}\int_\nu H_\nu \mathrm{d}\nu = -\int_\nu k_\nu (J_\nu - B_\nu)\mathrm{d}\nu = 0. \tag{8.20}$$

Therefore, we get that $\frac{\mathrm{d}F_{texttot}}{\mathrm{d}z} = 0$: flux is constant.

Let's do the same for the first moment.

$$\frac{1}{2}\int_{-1}^{1} \mu^2 \frac{\mathrm{d}I_\nu}{\mathrm{d}\tau_\nu}\mathrm{d}\mu = \frac{1}{2}\int_{-1}^{1} \mu I_\nu \mathrm{d}\mu - \mu B_\nu \mathrm{d}\mu. \tag{8.21}$$

(I think this is the same idea as in weak solutions of PDEs, where if something is a solution its integral against any test function will work out.) The last term is 0 because it's $\cos\theta$ over a circle, and we have exprssions for the other two:

$$\frac{\mathrm{d}K_\nu}{\mathrm{d}\tau_\nu} = H_\nu = \frac{F_\nu}{4\pi}. \tag{8.22}$$

For high τ, we have $I_\nu = I_0 + I_1\mu$, and for this case we can show $K_\nu = \frac{J_\nu}{3}$. If we assume this holds over the whole atmosphere, this is known as the Eddington approximation.

Under this approximation, we have

$$\frac{\mathrm{d}J_\nu}{\mathrm{d}\tau_\nu} = \frac{3F_\nu}{4\pi}. \tag{8.23}$$

For a gray atmosphere, we represent κ_ν by some mean opacity $\bar{\kappa}$ and we'll assume no scattering for now. Plug this back into the Eddington approximation, replacing $\mathrm{d}\tau = -\kappa\rho\mathrm{d}z$, and

$$\frac{1}{\bar{\kappa}\rho}\frac{\mathrm{d}J_\nu}{\mathrm{d}z} = -\frac{3}{4\pi}F_\nu. \tag{8.24}$$

Integrate over ν and we get

$$\frac{1}{\bar{\kappa}\rho}\frac{\mathrm{d}}{\mathrm{d}z}\int_0^\infty J_\nu \mathrm{d}\nu = -\frac{3}{4\pi}\int_0^\infty F_\nu \mathrm{d}\nu, \tag{8.25}$$

and since we're averaging and factoring out κ, the original RTE gives us

$$J = \int_\nu J_\nu \mathrm{d}\nu = \int_\nu B_\nu \mathrm{d}\nu = \frac{\sigma T^4}{\pi}. \tag{8.26}$$

This gives us

$$\frac{\mathrm{d}T}{\mathrm{d}z} = \frac{-3\bar{\kappa}\rho}{16\sigma T^3}F_{\text{tot}}. \tag{8.27}$$

Extrasolar Planets **Lent 2022**

Lecture 9: Temperature profile, convection

Lecturer: Nikku Madhusudhan *9 February* *Aditya Sengupta*

Last time, we found a differential equation in T, which we can try to solve to get the actual temperature dependence of the atmosphere. Replacing $F_{tot} = \sigma T_{eff}^4$, we get

$$\frac{\mathrm{d}\sigma T^4}{-\overline{\kappa}\rho \mathrm{d}z} = \frac{3}{4}\sigma T_{eff}^4, \tag{9.1}$$

and we get that

$$T^4 = \frac{3}{4}T_{eff}^4 \cdot \tau + C, \tag{9.2}$$

and by working out limits carefully we can get that $C = \frac{1}{2}T_{eff}^4$. Rearranging, we get

$$T^4 = \frac{3}{4}T_{eff}^4\left(\tau + \frac{2}{3}\right). \tag{9.3}$$

It's common in astronomy to set $\tau = \frac{2}{3}$ and to say this surface is the photosphere. If we do that here, we get $T = T_{eff}$, so we have flux equivalent to the blackbody of the same temperature.

When $\tau \to 0$, we get $T = T_{eff}/2^{1/4}$. This is known as the *skin temperature*: at the very top of the atmosphere, our assumptions break down, and this is a convenient point to look at to figure out where that happens.

In the high τ limit, we get $T^4 \propto \tau$. Putting all of this together, we get a $T - z$ graph that asymptotes towards a constant at high T and towards infinity at low T.

All of this was for an isolated atmosphere heated from below. Now, let's look at the case of an irradiated atmosphere. We have two sources of radiation: the planet and the star. The planet radiation peaks in IR wavelengths, whereas the stellar radiation will peak in optical wavelengths. We therefore need to choose two equivalent grey opacities and look at the interactions between them. We'll just cut to the chase and not go through the whole derivation.

This is still an approximate expression because we're assuming grey opacities, but we get

$$T^4 = \frac{3}{4}T_{int}^4\left(\tau + \frac{2}{3}\right) + \frac{3}{4}T_{irr}^4 f\left[\frac{2}{3} + \frac{1}{\gamma\sqrt{3}} + \left(\frac{\gamma}{\sqrt{3}} - \frac{1}{\gamma\sqrt{3}}\right)e^{-\gamma\tau\sqrt{3}}\right]. \tag{9.4}$$

T_{irr} is the temperature corresponding to the incident stellar flux, f corresponds to the fraction of incident energy retained, and $\gamma = \frac{\kappa_{\text{visible}}}{\kappa_{\text{thermal}}}$. Let's look at some asymptotic cases.

If $T_{irr} = 0$, we recover our internal flux expression. If the atmosphere is highly irradiated and if τ is sufficiently large (say above 10), $T_{irr} \gg T_{int}$ and the first term and the exponential term both drop out,

leaving us with $T \to$a constant determined by T_{irr}, f, γ. If $\tau \to 0$, we also get T going to a constant. What happens in between?

We can compute $\frac{\mathrm{d}T}{\mathrm{d}\tau}$:

$$\frac{\mathrm{d}T}{\mathrm{d}\tau} = \frac{3}{16}\frac{T_{int}^4}{T^3} + \frac{3}{16}\frac{T_{irr}^4}{T^3} f(1-\gamma^2)e^{-\gamma\tau\sqrt{3}}. \tag{9.5}$$

If $\gamma < 1$, we get $\frac{\mathrm{d}T}{\mathrm{d}\tau} > 0$ which implies $\frac{\mathrm{d}T}{\mathrm{d}z} < 0$. If $\gamma > 1$, we get the exact opposite: $\frac{\mathrm{d}T}{\mathrm{d}\tau} < 0$ and $\frac{\mathrm{d}T}{\mathrm{d}z} > 0$. Either way, we have a nonzero slope between two isotherms. This is a *thermal inversion*.

The conditions on this are high irradiation (meaning this doesn't happen in the solar system) and high $\frac{\kappa_{vis}}{\kappa_{th}}$. If visible opacity is greater than thermal opacity, the visible opacity captures the light coming from above and reradiates it, causing a thermal inversion at the top. In future lectures, we'll look at the conditions within atmospheres for this to hold.

For now, let's look at a different mode of energy transport: convection. Take a bubble of gas and displace it by a distance $\mathrm{d}z$. Does it keep rising or does it come back? This can tell us about the stability of gases in the atmosphere.

Let's build a model for convective transport. Say our bubble is in thermal equilibrium. We'll describe the bubble initially by ρ_i^b, T_i^b, P_i^b and the surroundings initially by ρ_i^s, T_i^s, P_i^s. Initially, the temperature and pressure are about the same for the bubble and the surroundings, which means by the ideal gas law so is the density. In the final state, we know that $P_f^s = P_f^b$, and let's require that the bubble has to keep floating. Buoyancy tells us that $\rho_f^b < \rho_f^s$, so the ideal gas law again tells us that $T_f^b > T_f^s$. Putting differentials on, we can say

$$\frac{\mathrm{d}T^b}{\mathrm{d}z} > \frac{\mathrm{d}T^s}{\mathrm{d}z} \tag{9.6}$$

$$\underbrace{\frac{\mathrm{d}T^s}{\mathrm{d}T}}_{\text{atmos}} < \frac{\mathrm{d}T^b}{\mathrm{d}z}. \tag{9.7}$$

This gives us a condition for a convective instability,

$$\left.\frac{\mathrm{d}T}{\mathrm{d}z}\right|_{\text{atmos}} \leq \left.\frac{\mathrm{d}T}{\mathrm{d}z}\right|_{ad}. \tag{9.8}$$

We can make this a more explicit expression. The bubble undergoes adiabatic expansion, which we can express using

$$P\rho^{-\gamma} = \text{const} \tag{9.9}$$

$$\frac{\mathrm{d}P}{P} = \frac{\mathrm{d}\rho}{\rho} + \frac{\mathrm{d}T}{T} \tag{9.10}$$

$$\frac{\mathrm{d}P}{\mathrm{d}z} = -\rho g. \tag{9.11}$$

Putting these together, we get

$$\left.\frac{\mathrm{d}T}{\mathrm{d}z}\right|_{\mathrm{ad}} = -\frac{g}{c_p}. \tag{9.12}$$

Extrasolar Planets **Lent 2022**

Lecture 10: Convection, thermal inversions

Lecturer: Nikku Madhusudhan *11 February* *Aditya Sengupta*

10.1 Recap

We've been looking at the temperature profiles for various atmospheric structures. Last time, we looked at the case of an isolated atmosphere heated from below, and we found

$$T^4 = \frac{3}{4}T_{eff}^4\left(\tau + \frac{2}{3}\right). \tag{10.1}$$

We'll take a quick sidebar to show where we got the constant $\frac{2}{3}$. Let's compute the emergent flux, or surface flux, in this case. We previously showed this is

$$F_\nu = 2\pi\int_0^1 I_\nu \mu \mathrm{d}\mu = 2\pi\int_0^1\int_0^\infty B_\nu e^{-\tau/\mu}\mathrm{d}\tau\mathrm{d}\mu. \tag{10.2}$$

Integrating this over all frequencies, we get

$$F = \int_0^\infty F_\nu \mathrm{d}\nu = 2\pi\int_0^1\int_0^\infty \underbrace{\int_0^\infty B_\nu \mathrm{d}\nu}_{J} e^{-\tau/\mu}\mathrm{d}\tau\mathrm{d}\mu. \tag{10.3}$$

Making some further substitutions, we get

$$F = 2\pi\int_0^1\int_0^\infty \left(\frac{3}{4\pi}F\tau + A\right)e^{-\tau/\mu}\mathrm{d}\tau\mathrm{d}\mu. \tag{10.4}$$

This can be solved analytically to get simply $A = \frac{F}{2\pi}$, which we can plug back in to the temperature profile to get

$$J = \frac{3}{4\pi}F\tau + \frac{F}{2\pi} = \frac{3}{4\pi}F\left(\tau + \frac{2}{3}\right). \tag{10.5}$$

10.2 Irradiated atmospheres

Next, we looked at the irradiated atmosphere, where we saw

$$T^4 = \frac{3}{4}T_{int}^4\left(\tau + \frac{2}{3}\right) + \frac{3}{4}T_{irr}^4 f\left[\frac{2}{3} + \frac{1}{\gamma\sqrt{3}} + \left(\frac{\gamma}{\sqrt{3}} - \frac{1}{\gamma\sqrt{3}}\right)e^{-\gamma\tau\sqrt{3}}\right] \tag{10.6}$$

where $T_{irr}^4 = T_s^4 \frac{R_s^2}{a^2}$. This made sense in some limits, and we made a qualitative plot of the behaviour, which showed thermal inversion: a monotonic change between two isotherms. In practice, at high pressures and τ values, it starts levelling off again after the second isotherm as the atmosphere becomes convective, but we'll never observe that high.

10.3 Convection

We came up with a condition for convective instability, which from adiabatic theory comes out to

$$\left.\frac{\mathrm{d}T}{\mathrm{d}z}\right|_{atm} \leq \frac{-g}{c_p}, \tag{10.7}$$

and we can associate this with the expression we came up with before,

$$\frac{\mathrm{d}T}{\mathrm{d}z} = -\frac{3K\rho}{16T^3}T_{int}^4. \tag{10.8}$$

This means as we go deeper into the atmosphere, ρ increases, and at some pressure sufficiently large, we enter the convective regime and the above condition is satisfied. All profiles eventually become convective.

Note that thermal inversions are necessarily radiative, because they need $\left.\frac{\mathrm{d}T}{\mathrm{d}z}\right|_{atm} > 0$, but those planets' temperature profiles go convective below that inversion. It's possible to not have a second isotherm, and to have the radiative-convective boundary exactly at the end of the thermal inversion. The edge of a thermal inversion that either gives way to a second isotherm or the convective zone is usually around 0.1 bar.

All solar system planets larger than Earth have thermal inversions, because they have sufficient irradiation from the Sun (although it's not huge) and some source of visible opacity intercepting and reradiating the stellar irradiation. On Earth, this source is ozone, and on other planets there's various hydrocarbons.

10.4 Theory of thermal inversions

In order to get a thermal inversion, we need $\frac{\mathrm{d}T}{\mathrm{d}\tau} < 0$, which we can get if T_{irr} is significant/high and if $\gamma > 1$.

If you just saw the solar system planets, you'd see thermal inversions everywhere, so you'd think that would be the norm. But the molecular species causing the required high opacity varies widely within the solar system: on Earth, it's caused by ozone, which isn't present in other solar system atmospheres, because the molecules like ozone that we see causing thermal inversions in the solar system are low-temperature molecules, so they won't be present in hot Jupiters. Hubeny et al., 2003, suggested that on Jupiter it was caused by TiO/VO.

Extrasolar Planets **Lent 2022**

Lecture 11: Thermal inversions, pressure, chemistry

Lecturer: Nikku Madhusudhan *14 February* *Aditya Sengupta*

11.1 Thermal inversions: research retrospective

We're continuing our study of thermal inversions, specifically in hot Jupiters as they're highly irradiated. Previously, we saw that inversions can be caused by titanium oxide and vanadium oxide at high temperatures, because they've been seen in very hot brown dwarfs. Initially, it was thought there was a cutoff incident flux below which there wouldn't be thermal inversions (Fortney et al., 2008), but they found planets below that cutoff that did show thermal inversions, and planets above it that didn't. A possible explanation (Spiegel et al., 2009) was that TiO and VO were depleted by gravitational settling and condensation. Knutson et al. tried to correlate these observations to stellar activity (the thinking being that more active stars would be more likely to dissociate atmospheric species) with some success. Next, Madhusudhan et al. 2011 (743, 191) found a correlation between thermal inversions and C/O content, but it wasn't definitive. Then, it was found that HD 209458b didn't have a thermal inversion at all! For strong spectroscopic evidence of a thermal inversion, we needed to go *very* hot; WASP-33b is a few thousand Kelvin and showed this evidence. Since then, we've found thermal inversions in several *ultra*-hot Jupiters.

We've looked at ways of inducing a thermal inversion that focus on increasing κ_{vis}, with species like TiO, so potential new research directions include: add in other sources of visible opacity, or lower κ_{th}. Both of these will have a net effect of increasing γ. We've found more species that cause both of these, and this is an open area of research.

11.2 Pressure

Previously, we used pressure in deriving the convective equilibrium condition, by assuming hydrostatic equilibrium: $\frac{\mathrm{d}P}{\mathrm{d}z} = -\rho g$. To solve this, we introduce an equation of state, which in this case is simply the ideal gas law $P = \frac{\rho}{\mu_m} k_b T$. Substituting back in, separating, and integrating, we get

$$\int_{P_0}^{P} \frac{\mathrm{d}P'}{P'} = -\int_{z_0}^{z} \frac{\mu_m g}{k_b T(z)} \mathrm{d}z. \tag{11.1}$$

We can precisely solve this for the isothermal case:

$$\int_{P_0}^{P} \frac{\mathrm{d}P'}{P'} = -\frac{\mu_m g}{k_b T}(z - z_0) \tag{11.2}$$

$$P = P_0 e^{-\frac{z-z_0}{H_{sc}}}, \tag{11.3}$$

where the scale height H_{sc} is given by $H_{sc} = \frac{k_b T}{\mu_m g}$. Otherwise, the most general expression we can write down is

$$P(z) = P_0 e^{-\frac{\mu_m}{k_b}} \int_{z_0}^{z} \frac{g(z')}{T(z')} \mathrm{d}z', \tag{11.4}$$

and we can get $\rho(z)$ just from plugging back into the ideal gas law. We can determine z_0 by noting the maximal optical depth we can probe to in secondary eclipse, and we can let P_0 be a free parameter that we fit to the data.

11.3 Atmospheric chemical compositions

There's broadly two types of planets: rocky and giant. Giant planets have primary atmospheres, meaning they're hydrogen-dominated: mostly H2 and a bit of He. This is because they come from the retention of primordial atmospheres. As planets get bigger and bigger, they undergo what's called *runaway accretion* from the nebula from which they form, and they retain much of the nebula's hydrogen envelope. This is why giant planets have large hydrogen-rich atmospheres. We can still have more complex molecules, but they're in chemical equilibrium and much smaller abundances. By contrast, rocky planets have heavier molecular atmospheres: N2, O2, CO2 on Earth and Venus, for example. The reason for this is they're all secondary atmospheres. Rocky planets are smaller, so they have lower gravities and lose much of their hydrogen envelopes over geological timescales. As a result of their small size, there's interactions that can no longer be ignored, so secondary atmospheres are mostly in disequilibrium.

Extrasolar Planets **Lent 2022**

Lecture 12: Chemical composition of atmospheres

Lecturer: Nikku Madhusudhan *16 February* *Aditya Sengupta*

Between giant planets and rocky planets, the atmospheres are significantly different. We broadly say that giant planets have primary atmospheres and are H2 rich, whereas rocky planets have secondary atmospheres which have a variety of compositions: N2, O2, CO2, and so on. Giant planets generally have atmospheres in chemical equilibrium, and rocky planets generally don't, as there are atmospheric processes forcing it out of chemical equilibrium.

The problem statement, when we're talking about chemistry, is this: you have a box of gas (the system is idealised) into which we throw some elements. You maintain the box at a constant pressure and temperature. As time goes on, what happens inside the box? Do the elements stay atomic, or do they form molecules?

In mechanical systems, we find long-run behaviour by looking for low-energy states. In a chemical system, you do this by minimising the Gibbs free energy. Why is that the case?

We'll start from the first law of thermodynamics.

$$\mathrm{d}U = \mathrm{d}Q - \mathrm{d}W = \mathrm{d}Q - P\mathrm{d}V. \tag{12.1}$$

We want to see what happens to the Gibbs potential in a closed system.

$$G = H - TS = U + PV - TS. \tag{12.2}$$

This is a measure of the energy content in the system, minus its disorder. You want to minimise H and maximise S. Let's look at the change in Gibbs free energy.

$$\begin{aligned}\mathrm{d}G &= \mathrm{d}U + P\mathrm{d}V + V\mathrm{d}P - T\mathrm{d}S - S\mathrm{d}T &(12.3)\\ &= \mathrm{d}Q - P\mathrm{d}V + +P\mathrm{d}V + V\mathrm{d}P - T\mathrm{d}S - S\mathrm{d}T &(12.4)\\ &= \mathrm{d}Q + V\mathrm{d}P - T\mathrm{d}S - S\mathrm{d}T. &(12.5)\end{aligned}$$

Now, let's look at the second law: $\mathrm{d}S \geq \frac{\mathrm{d}Q}{T}$. Plug that in to get

$$\mathrm{d}G \leq T\mathrm{d}S + V\mathrm{d}P - T\mathrm{d}S - S\mathrm{d}T = V\mathrm{d}P - S\mathrm{d}T. \tag{12.6}$$

If we maintain the box at a constant pressure and temperature, we get that $\mathrm{d}G \leq 0$. The equilibrium condition is $\mathrm{d}G = 0$, and otherwise it'll reduce. For any chemical reaction, $\mathrm{d}G < 0$, so chemical systems tend to minimise G.

Let's look at a box of gas with various species inside it. To start with, take the case of a single-component system, $\mathrm{d}G = V\mathrm{d}P - S\mathrm{d}T$. Hold T constant to get

$$\mathrm{d}G = V\mathrm{d}P = \frac{NRT}{P}\mathrm{d}P \tag{12.7}$$

$$G = G_N + NRT\ln\frac{P}{P_0}. \tag{12.8}$$

where $G_N = NG^0$ is the reference Gibbs free energy, and G^0 is that per mole.

$$G = N\left[G^0 + RT\ln(P/P_0)\right]. \tag{12.9}$$

If we do this for a system with multiple species, we add a bunch of these terms together:

$$G = \sum_i N_i\left[G_i^0 + RT\ln\frac{P_i}{P_0}\right]. \tag{12.10}$$

In the example sheet, we'll do this one step further by replacing the partial pressure by a mixing ratio.

$$G = \sum_i N_i\left[\frac{G_i^0}{RT} + \ln\frac{P}{P_0} + \ln f_i\right], \tag{12.11}$$

where f_i is the mixing ratio.

In this minimisation, P, T, and elemental (not molecular!) abundances are all fixed. We apply the molecular constraint by saying $\sum_i a_{ij}n_i = b_j$, where i runs over the molecules and j over the atoms. a_{ij} is the number of atoms of type j in molecule i, n_i is the number of moles of molecule i, and b_j is the number of moles of element j. The mixing ratios are the only free parameter that we run the minimisation over.

Let's look at a qualitative example. In H-rich atmospheres, one of the main reactions is $\mathrm{H} + \mathrm{H} \longleftrightarrow \mathrm{H_2}$. In carbon-rich atmospheres, you encounter $\mathrm{CO_2} + 3\,\mathrm{H_2} \longleftrightarrow \mathrm{CH_4} + \mathrm{H_2O}$, and in nitrogen-rich atmospheres, you encounter $\mathrm{N_2} + 3\,\mathrm{H_2} \longleftrightarrow 2\,\mathrm{NH_3}$. (See diagrams on ipad) For the carbon reaction, we can plot G/RT against T and get roughly increasing curves, and find that there's a change in which side is favoured at around 400K. To the left of the change (at low temperatures), $\mathrm{CH_4}$ is favored, which is backed up by the detection of methane in Jupiter through Neptune, and to the right, $\mathrm{CO_2}$ is favored, which is backed up by its detection in hot Jupiters and the lack of detections of methane in those atmospheres. Similarly, the nitrogen transition point is around 500K at 1 bar.

We can also look at the reaction rate. If we have a reaction $\mathrm{A} + \mathrm{B} \longleftrightarrow \mathrm{C} + \mathrm{D}$ with forward rate k_f and reverse rate k_r, we can write down

$$\frac{\mathrm{d}[A]}{\mathrm{d}t} = k_r[C][D] - k_f[A][B], \tag{12.12}$$

and this is 0 at chemical equilibrium. We can write

$$\frac{k_f}{k_r} = \frac{[C][D]}{[A][B]} \tag{12.13}$$

and at equilibrium, we also have $\Delta G = 0$, or $G_A + G_B - G_C - G_D = 0$. Using this combined with the earlier expression for G, we can find

$$\Delta G = \Delta G^0 + RT \ln \frac{[A][B]}{[C][D]} \tag{12.14}$$

where ΔG^0 is the change in Gibbs free energy at a reference pressure. This gives us

$$\frac{k_f}{k_r} = e^{\Delta G^0 / RT}. \tag{12.15}$$

We can therefore calculate either the forward or the reverse reaction rate from just the other one and from ΔG^0.

Extrasolar Planets **Lent 2022**

Lecture 13: Chemical equilibrium and disequilibrium

Lecturer: Nikku Madhusudhan *18 February* *Aditya Sengupta*

13.1 Equilibrium chemistry

We've been looking at chemical equilibrium in planetary atmospheres, in terms of the Gibbs free energy and the common reactions in hydrogen-rich atmospheres. We saw there are profiles that are dominated by CO (high temperature) and those that are dominated by CH_4 (low temperature), and we'll see that we can get non-equilibrium chemistry in the region that interpolates between them.

As a summary of chemistry in hydrogen-rich atmospheres:

- Water should be the dominant O carrier at all temperatures
- CO should be the dominant C carrier at high temperatures
- CH_4 should be the dominant C carrier at low temperatures
- Similarly, NH_3 at low temperatures and N_2 at high temperatures

As metallicity increases, all molecules become more abundant, especially heavier ones. Other species also become more prominent in hot atmospheres; for instance, we saw TiO and VO are important to thermal inversions, and people have both theoretically predicted and actually observed atomic Na and K.

If we increase the C/O ratio, the mixing ratio of water drops drastically, and the leftover oxygen binds with carbon to create higher abundances of CO and other hydrocarbons. This is specifically a high-temperature effect, because otherwise methane takes all the carbon. Water remains pretty constant at low temperatures irrespective of the C/O ratio, but CO becomes more abundant than methane at some point and we start seeing more significant effects. The threshold is somewhere around 0.7-0.8.

Most hot Jupiters are over 1200K, so the measurement of water in HJs is a very good diagnostic of the C/O ratio. This can be corroborated by looking for hydrocarbons, but just measuring water and finding that it's two orders of magnitude below the solar abundance narrows down the possibilities to very low metallicity or high C/O ratio. Generally, the former is considered impractical.

In recent years, it's become evident that there's other influences on water abundances. We've found a population of extremely irradiated *ultra* hot Jupiters. At these temperatures (around 2500K) we should expect that many species thermally dissociate. This happens for water faster than CO, but if you go hot enough, all the common molecules are dissociated and their abundances are lower. Ions and free metallic atoms (Fe, Cr, etc) start becoming more chemically abundant, and we may get significant opacity from sources like H^-. In the ultimate limit, you get to the same as observations for stars, where there are no molecules and instead just atoms.

Let's look at a few observations. In the gaseous and ice planets, we've detected methane and ammonia, and a few hydrocarbons, which is consistent with what we expect from low-temperature chemistry. We don't detect much water as it's often frozen out, but water is the most commonly seen molecule in giant exoplanets. These are consistent with what we expect in theory. It's well known that we can find Na, K,

TiO in hot Jupiters, and we've made atomic detections in ultra hot Jupiters, of which a principal example is KELT-9b. Today, we have populations of species across many different planets, going down to Neptunes and mini-Neptunes.

13.2 Non-equilibrium chemistry

We alluded to the transition region between CO and CH_4 earlier. What happens when we have a temperature profile that crosses the boundary between the two regimes? If you have strong vertical mixing in the atmosphere, we can dredge up some of the CO from the bottom of the atmosphere to the top. We usually can't see far enough into the atmosphere that we would be able to see significant CO abundances, but with this effect, we'd be able to see both. If you look at a cool planet and see CO in its atmosphere, that's a signal of strong vertical mixing.

The CO-CH_4 equilibrium is composed of a chain of reactions, and people have identified the rate-limiting step: $H_2 + CH_2OH \longrightarrow CH_3OH + H$. This gives us the chemical timescale

$$\tau_{\text{chem}} = \frac{[\text{CO}]}{-\frac{\text{d}[\text{CO}]}{\text{d}t}} = \frac{[\text{CO}]}{k_{f,N}[\text{H}_2][\text{CH}_3\text{O}]} \tag{13.1}$$

where $k_{f,N}$ can be derived experimentally and the abundances can be obtained from chemical equilibrium calculations. This chemical timescale has to compete with the mixing timescale,

$$\tau_{\text{mix}} = \frac{L^2}{K_{zz}}, \tag{13.2}$$

where the mixing length L is usually taken as 0.1 times the scale height and K_{zz} determines the strength of mixing. The condition for vertical mixing is $\tau_{\text{mix}} \leq \tau_{\text{chem}}$, and the intersection of the two curves (on a plot of pressure against the time) is the point at which the concentrations of species are *quenched* (frozen), and they'll remain there unless other disequilibrium processes set in. τ_{chem} increases fairly monotonically with pressure, whereas τ_{mix} does not vary much with varying pressure. For CO, they cross at 30 bars.

In exoplanets, one of the early studies of non-equilibrium chemistry was in studying the hot Neptune GJ 436b. Strong CO absorption was observed, but its temperature structure didn't seem to support that, so one argument was strong vertical mixing along with high metallicity.

There is one other mechanism of non-equilibrium chemistry: photochemistry, which we'll look at next lecture.

Extrasolar Planets **Lent 2022**

Lecture 14: Photochemistry

Lecturer: Nikku Madhusudhan *21 February* *Aditya Sengupta*

We're continuing our discussion of chemistry, focusing on photodissociation of species. If you go high enough in the atmosphere, the incoming radiation photodisassociates the molecules, leaving them in their atomic/ionic forms. Going even further up, you have atmospheric escape.

We quantify all these through the *continuity equation*,

$$\partial n_i t + \partial \Phi_i z = P_i - L_i. \tag{14.1}$$

and through the reaction rates for thermochemical and photochemical reactions, respectively

A + B $\longrightarrow$ C + D

$$\frac{\mathrm{d}[A]}{\mathrm{d}t} = -k[A][B], \frac{\mathrm{d}[C]}{\mathrm{d}t} = k[A][B] \tag{14.2}$$

and

A + hν $\longrightarrow$ C + D

$$\frac{\mathrm{d}[A]}{\mathrm{d}t} = -J[A], \frac{\mathrm{d}[C]}{\mathrm{d}t} = J[A]. \tag{14.3}$$

The bond energies of molecules are typically in the UV range, so ν should be ultraviolet. Photochemistry gets less and less efficient deeper in the atmosphere because it's used higher up to dissassociate the molecules in the upper atmosphere.

We define the photodissocation coefficient J in analogy with k, and it's a function of the molecular cross-section and the incident radiation flux.

These simple forms give us a large network of partial differential equations which we simultaneously solve for an atmospheric composition over time and altitude. See Moses et al., 2011, for a set of 90 molecules with 1600 reactions.

What is the emergent behaviour? If you go high up enough, everything gets photochemically dissociated. A bit below that, though, you'll get photochemically added byproducts, meaning there's more species observable in the atmosphere. Eventually, even those byproducts are dissociated, but there's an interplay between radiation and atmospheric chemistry. Further, these species can be considered tracers of photochemical activity: if we go deep enough, we'll observe them in steady state.

We can now identify three regimes of chemistry in planetary atmospheres.

- At $P \sim 1$ bar, in the lower atmosphere, equilibrium chemistry holds. P, T, ρ are all high enough that the reaction timescales are very short, so the thermochemical reaction rates are sufficiently short so as to allow equilibrium.
- At $P \sim 10^{-3}$ bar, non-equilibrium chemistry due to vertical mixing becomes important. Specific dynamics depend on K_{zz}, temperature, metallicity, and so on.

- At $P \sim 10^{-6}$ bar, non-equilibrium due to photochemistry becomes important, because incident irradiation is the most significant here.

This gives us an agenda for studying spectra: how do we use them as a probe with which to study all the physical and chemical processes in planetary atmospheres?

As an example of photochemistry, let's look at Earth's ozone layer. We'll look at a set of reactions called the Chapman reactions:

$\mathrm{O_2 + h\nu \longrightarrow O + O}$, $k_1 \equiv J_1$ $\mathrm{O + O_2 \xrightarrow{M} O_3}$, k_2 $\mathrm{O_3 + h\nu \xrightarrow{uv + vis} O + O_2}$, $k_3 \equiv J_3$ $\mathrm{O + O_3 \longrightarrow O_2 + O_2}$

and the reaction rates are determined by the photodissociation coefficient,

$$J_i(z) = \int_\nu \sigma_{i\nu} F_\nu e^{-\tau_\nu(z)/\mu} \mathrm{d}\nu, \tag{14.4}$$

and the known values

$$k_2 = 6 \times 10^{-34} \left(\frac{\tau}{300}\right)^{-2.3} \mathrm{cm^2/s} \tag{14.5}$$

$$k_4 = 8 \times 10^{-12} e^{-2060/T} \mathrm{cm^2/s}. \tag{14.6}$$

We can write out reaction rate equations in terms of these coefficients and these abundances,

$$\frac{\mathrm{d}[O]}{\mathrm{d}t} = 2k_1[O_2] - k_2[O][O_2][M] + \ldots \tag{14.7}$$

$$\frac{\mathrm{d}[O_3]}{\mathrm{d}t} = k_2[O][O_2][M] - k_3[O_3] - k_4[O][O_2] \tag{14.8}$$

For photochemical equilibrium, we want both of these to be 0, so enforcing that gives us

$$[O] = \frac{k_1[O_2]}{k_4[O_3]} \tag{14.9}$$

$$[O_3] = \frac{k_2[O][O_2][M]}{k_3 + k_4[O]} \tag{14.10}$$

By looking up precise numbers, we can show that $k_3 \gg k_4[O]$, which implies

$$[O_3] = \frac{k_2}{k_3}[O][O_2][M]. \tag{14.11}$$

If we substitute for [O], we get

$$[O_3] = \sqrt{\frac{k_1 k_2[M]}{k_3 k_4}}[O_2]. \tag{14.12}$$

At high z, $[O_2]$ decreases exponentially, so we get low O_2 and therefore low O_3. At low z, you can't use photochemical arguments: k_1 is small because of low flux, so we get low O_3 again. So where is the ozone? It must be somewhere in the middle (it's being produced, so it has to be somewhere) which is why you have an ozone layer. In the Earth's atmosphere, this happens at about 20-30km, or $P \sim 0.1$ bar, about where we have the thermal inversion.

Extrasolar Planets **Lent 2022**

Lecture 15: Atmospheric escape

Lecturer: Nikku Madhusudhan *23 February* *Aditya Sengupta*

We've looked at various chemical processes as a function of altitude, but we haven't yet really studied the mechanism by which atmospheric escape takes place. The simplest escape mechanism happens when particles have a velocity higher than the planet's escape velocity; that is, the *thermal escape mechanism*. In thermal equilibrium, particles follow a Maxwellian distribution,

$$f(u)\mathrm{d}u = n\left(\frac{2}{\pi}\right)^{1/2}\left(\frac{m}{k_BT}\right)^{3/2}u^2e^{-mv^2/2k_BT}\mathrm{d}v \tag{15.1}$$

This distribution peaks at $v_p = \sqrt{\frac{2k_BT}{m}}$, and we want to compare this to $v_{esc} = \sqrt{\frac{2Gm_p}{R_p}}$. Generally, to see non-negligible atmospheric escape, we want some cutoff on the high-velocity tail of the distribution; a common cutoff is $6v_p \geq v_{esc}$.

$$v_p \geq \frac{1}{6}\sqrt{\frac{2Gm_p}{R_p}} \tag{15.2}$$

Another thing to look at is the *exobase*: the location in the atmosphere where the mean free path $l = \frac{1}{n\sigma}$ exceeds the scale height $H_{sc} = \frac{k_BT}{m_pg}$. If $l > H_{sc}$, we have a collisionless atmosphere.

We can write down the rate of escape, or the Jeans escape flux:

$$\Phi = \frac{n_{exo}}{2\sqrt{\pi}}B\sqrt{\frac{2k_BT}{m}}(1+\lambda_{esc})e^{-\lambda_{esc}}, \tag{15.3}$$

where $B \sim 0.5 - 0.8$ is a factor accounting for repopulation time, and the escape parameter λ_{esc} is given by

$$\lambda_{esc} = \frac{Gm_pm}{R_{exo}k_BT}. \tag{15.4}$$

For $\lambda_{esc} \gg 1$, we get the so-called hydrostatic regime of escape.

Another escape mechanism is hydrodynamic escape, which is what happens when the atmosphere is heated with very energetic stellar extreme UV flux. Particles escape so fast that the atmosphere behaves like a dense fluid expanding outwards. Lighter particles (H) escape due to high UV, and heavier particles are entrained in the hydrodynamic flow of the lighter particles.

A third escape mechanism is energy-limited escape. The potential energy of the atmosphere in the planet's gravity is $E_p = \frac{-GM_pm_{atm}}{\beta R_p}$, and the power due to EUV is $P_{EUV} = \pi R_p^2F_{EUV}$. We can divide these to get a timescale for energy-limited escape:

There's a few non-thermal mechanisms too!

1. **Charge exchange**: collisions between highly energetic ions and neutral atoms. Charges exchange and impart kinetic energy to neutral atoms.
2. **Ion escape**: ions escape along open magnetic field lines. This is most efficient at the poles, which is why on Earth we have the phenomenon of polar wind.
3. **Stellar wind sweeping**: solar wind can sweep away ions in planetary atmospheres, especially in the absence of a planetary magnetic field.
4. **Sputtering**: fast-moving atoms come from outside the atmosphere, hit particles in the atmosphere and on the surface, and cause a cascade of high-velocity collisions.

Hydrodynamic escape is thought to be dominant, because of the large exospheric envelopes that have been detected. You can detect exospheres by seeing escape of Lyman-α photons.

Extrasolar Planets **Lent 2022**

Lecture 16: Clouds and hazes

Lecturer: Nikku Madhusudhan *25 February* *Aditya Sengupta*

We're almost done with atmospheres, but we haven't yet covered clouds and hazes or atmospheric circulation.

The first thing that comes to mind with clouds is condensation. The atmospheric temperature becomes less than the condensation temperature of the particles, so we have suspensions of liquid particles in gases.

When we talk about clouds, we're generally talking about condensates. Formally, we'll say a cloud is a mass of liquid or solid particles suspended in a planetary atmosphere, caused by condensation of atmospheric gases. Our principal example is water clouds in Earth's atmosphere.

Hazes are similar, but they don't occur from condensation. They consist of very small particles suspended in an atmosphere caused by photochemistry. For example, long-chain hydrocarbons in cold giant planet atmospheres from methane photochemistry.

Condensates (like water in Jupiter's atmosphere, or salt/metallic clouds in hotter atmospheres) get "frozen out" from being visible in spectra. Marley and Robinson 2014, good reference for cloud curves on a P-T diagram. Morley et al 2013 too.

What do clouds do to incident radiation? Mostly, scattering, and this is why I've been doing all this Mie theory reading and programming. There's two types of scattering, depending on the size of your particle a relative to the wavelength λ of the incident light.

1. When you have $a \ll \lambda$, you get Rayleigh scattering. In the limit, you get the same scattering that you would have from gas particles, and it's the same processes that cause the sky to be blue on Earth. $\sigma_\lambda \propto \frac{1}{\lambda^4}$, so there's more scattering the bluer you go. You don't necessarily need clouds or hazes to get Rayleigh scattering; in spectra, regardless of the presence or absence of clouds, you'll see a slope. A transmission spectrum (Δ vs λ) goes up as λ goes down if you start on the left end. The reason for this is in the small-particle limit, the incident EM wave is polarising the particles and creating a dipole that radiates with a certain frequency.
2. When you have $a \gtrsim \lambda$, you get Mie scattering. Mie theory gives you solutions to Maxwell's equations. The interaction of a plane wave with a particle using the particle as boundary conditions. I'd love to do some visualisations of Mie theory against Rayleigh scattering in the context of their impact on spectra, but I do not have the bandwidth right now; I'll see if I can make that part of the essay. When $a \gg \lambda$, Mie theory tends to geometric optics, and when $a \ll \lambda$, it tends to Rayleigh scattering.

Refs: Pinhas and Madhusudhan 2017, Wakeford and Sing 2015.

When you look at a spectrum, what do you actually see? Take a transmission spectrum with a Rayleigh scattering feature at small λ, and add in a cloud deck at a high point in the atmosphere greater than the scale height H. If the cloud were opaque at all features, the spectrum would become flat as the cloud would dominate. For a lower cloud deck, only some features would be muted. Clouds therefore cause muted features in IR spectra (as that's where absorption features are). Another impact is non-Rayleigh features or slopes in the visible regime.

In emission (secondary eclipse) spectra, a sufficiently high cloud deck masks out spectral features and replaces them with an equivalent blackbody spectrum. In general, you see muted spectral features here too.

Also, the impact of reflected light from the star goes up at lower wavelengths, as the star's blackbody peaks in the optical. This is what's known as the planetary *albedo*.

You can constrain the degeneracy between clouds vs. a genuine non-detection by looking at the optical and seeing if there's a Rayleigh feature or not, as well as by looking for multiple features instead of just a particular one.

There's a couple different kinds of albedos. The bond albedo A_B is the ratio of reflected light to incident light, integrated over frequency or wavelength. The geometric albedo A_G is the ratio of reflected light from the object at full phase (when the disk is fully illuminated) relative to that by a Lambertian surface of equal size at the same distance for a given wavelength. (A Lambertian surface is a surface with a flat brightness profile.)

$$\left.\frac{F_{p,\lambda}}{F_{s,\lambda}}\right|_{\oplus} = A_{G,\lambda}\frac{R_p^2}{a^2}. \tag{16.1}$$

The planet-star flux ratio in the optical gives us a good measurement of the geometric albedo.

GJ 1214 b.

Extrasolar Planets **Lent 2022**

Lecture 17: Atmospheric models

Lecturer: Nikku Madhusudhan *28 February* *Aditya Sengupta*

(I didn't write much on this day because I wanted to listen really closely)

When you're trying to make a model spectrum to compare to data, you need a method of model generation that incorporates all the effects we've looked at. This basically involves solving a bunch of equations we've seen already as a coupled system: radiative transfer, equation of state, hydrostatic equilibrium, opacity relations, etc. In this setup, we end up squishing all the atmospheric dependence into a parameter κ_λ, which we derive using chemical equilibrium. We impose that using a whole parallel chemical simulation module.

κ_λ in particular depends quite heavily on molecular absorption cross-sections, especially in the infrared. Therefore, molecular spectroscopy acts as a tracer of atmospheric processes. There are three observables in a spectrum: chemical compositions, temperature profiles, and energy budget.

What happens when you're matching a model to data, but the actual physics violates the assumptions you made in a self consistent model? Also, running self-consistent models takes time, and it takes too long to rerun them enough times to have them match data.

Back in 2008, we couldn't fit models to data very well; the initial water vapor detections had large error bars and wouldn't now be considered robust, as they're maybe only 1-2 σ. Another key problem was: do the models *uniquely* fit the data?

Extrasolar Planets **Lent 2022**

Lecture 18: 3D atmospheric efects

Lecturer: Nikku Madhusudhan *2 March* *Aditya Sengupta*

Atmospheres are three-dimensional, so for a full picture we have to run three-dimensional simulations. This gives rise to general circulation models. One of the main effects that are modelled is energy transport via winds, which is a necessarily 3D phenomenon.

GCMs essentially impose 3D versions of conservation equations (replace $\frac{\partial}{\partial z}$ with ∇ throughout, etc).

Although GCMs are pretty complicated to run, we can do some zeroth-order analysis. First, let's look at wind velocity. Between the day and night sides, let's say there's a temperature contrast ΔT. The zonal wind speed along the equator comes out to be $u \sim \sqrt{R\Delta T \Delta \ln P}$. The derivation will be left to an online reference, but we can plug in some reasonable numbers and get a sense of how big this is. If we take $R = 3700\,\mathrm{J/kg/K}$, $\Delta \ln P \sim 3$ and $\Delta T \sim 400$, then u comes out to around 2 kilometers per second.

How about the time scales on which dynamics change? There's two processes with competing time scales: radiative and advective cooling. For advective cooling, we can divide a length scale (the planetary radius) by the velocity we just derived, and we can get $\tau_{adv} \sim 10^5$s. How do you compare that to the radiative timescale? A radiative timescale basically measures how fast a perturbation in energy is radiated away. Add in energy per unit area $\Delta E = \rho c_p \Delta T \Delta z$. The advantage of taking a small slice Δz is you can assume it's a blackbody, so we get flux $\Delta F = \Delta(\sigma T^4) = 4\sigma T^3 \Delta T$. Dividing these out, we get

$$\tau_{rad} = \frac{\rho c_p \Delta z}{4\sigma T^3} \sim \frac{\Delta P}{g}\frac{c_p}{4\sigma T^3} \sim \frac{(\Delta P/1\mathrm{bar})}{(T/1000\mathrm{K})^3}\frac{3\times 10^5}{g/g_J}\mathrm{s}. \tag{18.1}$$

If you pick conditions such that $\tau_{rad} \ll \tau_{adv}$, you get large day-night contrast (and therefore a very high T), as excess energy is radiated away faster than it can be advected to the nightside. This is why hot planets have hotter daysides. Similarly, if you have $\tau_{rad} \gg \tau_{adv}$, the contrast is much smaller.

The band structure is determined by the Rhines length scale, which is the scale over which planetary rotation causes east-west jets. $L_\beta = \pi\sqrt{\frac{u}{\beta}}$, where $\beta = \frac{2\Omega\cos\varphi}{R_p}$ with φ = the latitude.

$$N \sim \frac{\pi R_p}{L_\beta} \sim \sqrt{\frac{2\Omega R_p}{u}} \tag{18.2}$$

For hot Jupiters, P is about a day, and $\Omega = \frac{2\pi}{P}$, and $u \sim 1$ km/s, so plugging everything in we get $N \sim 1-2$. For Jupiter, the same calculation gives us $N \geq 10$. Larger N gives us more banded structures.

To sum up, the key observational inferences are

1. Day-night contrast
2. Hot-spot offsets
3. Wind velocities

Extrasolar Planets **Lent 2022**

Lecture 19: Interiors

Lecturer: Nikku Madhusudhan *4 March* *Aditya Sengupta*

Look at the review paper on advective-radiative balance, as some terms may not have been totally clear from the lecture.

Let's look at exoplanetary interior properties. There isn't really anything that's observable other than the bulk properties (the mass and radius) and the atmospheric properties, so let's start working with those. We can write down conservation equations.

1. Conservation of mass: $\frac{\mathrm{d}m_r}{\mathrm{d}r} = 4\pi r^2 \rho(r)$
2. Force balance/hydrostatic equilibrium: $\frac{\mathrm{d}P}{\mathrm{d}r} = -\rho g = -\frac{Gm_r}{r^2}\rho(r)$.
3. Energy generation/conservation of angular momentum: $\frac{\mathrm{d}L_r}{\mathrm{d}r} = 4\pi r^2 \rho \dot{\epsilon}$, where $\dot{\epsilon}$ is the energy generation rate per unit mass.
4. Convective temperature gradient (active in most of the interior): $\frac{\mathrm{d}T_r}{\mathrm{d}r} = -\frac{Gm_r}{c_p r^2} = -\frac{g}{c_p}$ and radiative temperature gradient: $\frac{\mathrm{d}T_r}{\mathrm{d}r} = -\frac{3\bar{\kappa}\rho}{16\sigma T^3}F_{int} = -\frac{3\bar{\kappa}\rho}{16\sigma T^3}\frac{L_r}{4\pi r^2}$.
5. An equation of state, $P = P(\rho, T)$.

This is all pretty structurally similar to the analysis we ran for stars, with the key differences that $\dot{\epsilon}$ and the equation of state are very different.

We can look at polytropic examples and see if we can get some test cases for how these quantities vary. A polytropic relation is $P = K\rho^{\frac{1}{n}+1}$, where n is known as the *polytropic index*. Putting these together with mass conservation and hydrostatic equilibrium, we get

$$-\frac{\mathrm{d}}{\mathrm{d}r}\left(\frac{r^2}{\rho G}\frac{\mathrm{d}P}{\mathrm{d}r}\right) = 4\pi r^2 \rho \tag{19.1}$$

$$\frac{1}{r^2}\frac{\mathrm{d}}{\mathrm{d}r}\left[\frac{r^2}{\rho}\frac{\mathrm{d}P}{\mathrm{d}r}\right] = -4\pi G\rho. \tag{19.2}$$

By steps we'll do on our examples sheet, we get

$$\frac{1}{r^2}\frac{\mathrm{d}}{\mathrm{d}r}\left[\frac{r^2}{\rho}\frac{K(n+1)}{4\pi G}\frac{\rho^{1/n}}{n}\frac{\mathrm{d}\rho}{\mathrm{d}r}\right] = -\rho. \tag{19.3}$$

We further assume a form $\rho = \rho_c \theta^n(r)$, where ρ_c is the central pressure and θ is a dimensionless function defining the decay.

$$\frac{1}{r^2}\frac{\mathrm{d}}{\mathrm{d}r}\left[r^2\frac{K(n+1)}{4\pi G}\rho_c^{(1-n)/n}\frac{\mathrm{d}\theta}{\mathrm{d}r}\right] = -\theta^n. \tag{19.4}$$

Further, we set $r = \alpha\xi$, where α contains all the material properties.

$$\alpha^2 = \frac{K(n+1)}{4\pi G}\rho_c^{(1-n)/n}. \tag{19.5}$$

α has dimensions of length and ξ is dimensionless. After a lot more algebra, we get the *Lane-Emden equation*:

$$\frac{1}{\xi^2}\frac{\mathrm{d}}{\mathrm{d}\xi}\left[\xi^2\frac{\mathrm{d}\theta}{\mathrm{d}\xi}\right] = -\theta^n. \tag{19.6}$$

We can solve this for specific n. For $n = 0$, we get $\theta(\xi) = 1 - \frac{\xi^2}{6}$. Further, we can get boundary conditions by setting $\theta = 0$ and we recover the surface properties: in this case, $\xi_1 = \sqrt{6}$. For $n = 1$, we get $\theta = \frac{\sin\xi}{\xi}$ and $\xi_1 = \pi$. For $n = 5$, we get $\theta = \left(1 + \frac{\xi^2}{3}\right)^{-1/2}$ and $\xi_1 = \infty$.

If we have constant θ we can just recover the simple mass-radius relation $\rho = \rho_c = \frac{M}{R^3}$. For other polytropic cases, we can get a similar mass-radius relation.

$$\frac{\mathrm{d}M}{\mathrm{d}r} = 4\pi r^2\rho, r = \alpha\xi, \rho = \rho_c\theta^n. \tag{19.7}$$

Integrate for M and use the Lane-Emden equation to get

$$M = \int_0^R 4\pi r^2\rho\mathrm{d}r = 4\pi\alpha^3\int_0^{\xi_1}\rho_c\theta^n\xi^2\mathrm{d}\xi \tag{19.8}$$

$$M = 4\pi\alpha^3\rho_c\int_0^{\xi_1}\frac{\mathrm{d}}{\mathrm{d}\xi}\left[-\xi^2\frac{\mathrm{d}\theta}{\mathrm{d}\xi}\right]\mathrm{d}\xi \tag{19.9}$$

$$M = 4\pi\alpha^3\rho_c\left[-\xi^2\frac{\mathrm{d}\theta}{\mathrm{d}\xi}\right]_{\xi_1}. \tag{19.10}$$

Interestingly, we don't have to integrate for the mass, and instead we just need one evaluation at a point.

We can further get the radius,

$$R = \alpha\xi_1 = \sqrt{\frac{K(n+1)}{4\pi G}}\rho_c^{(1-n)/2n}\xi_1 \tag{19.11}$$

$$R^{3-n}M^{n-1} = \left(\frac{K}{GC}\right)^n. \tag{19.12}$$

For $n = 0$, we recover the desired behaviour of $R \propto M^{1/3}$.

Extrasolar Planets **Lent 2022**

Lecture 20: M-R relations, luminosity evolution

Lecturer: Nikku Madhusudhan *7 March* *Aditya Sengupta*

Previously, we solved the Lane-Emden equation and got the mass-radius relation $R \propto M^{(1-n)/(3-n)}$ for a polytrope of index n. If we take $n = 0$, we get $R \propto M^{1/3}$, which corresponds to a constant density interior, or an incompressible fluid. For planets, until a certain mass limit, this is an accurate M-R relation.

However, if we look at giant planets, this breaks down. Say $n = \frac{3}{2}$, then $\gamma = \frac{5}{3}$ and $R \propto M^{-1/3}$. This case corresponds to an adiabatic interior or degenerate (nonrelativistic) gas. When objects become very massive, the degeneracy pressure starts to become more important and eventually dominate, and we get the $n = \frac{3}{2}$ relationship.

We can interpolate between them to plot $\log R$ against $\log M$. We see that if it's sloping upward for small M and downward for large M (todo plot this), we see that there's a maximum somewhere in the middle. To find this precisely, we'd need to run more detailed models.

In practice, $n = 0$ and $n = \frac{3}{2}$ don't actually describe the interiors of planets, just simplified models. Here's a few actual n values from simulations in terms of masses:

M/M_J	n	$(1-n)/(3-n)$
0.1	0.6	0.16
1	1	0
10	13	-0.18

So the actual $\log R$ vs $\log M$ curve isn't as steep as our previous assumptions would suggest.

Let's look at a more complete picture for general hydrogen-rich objects, shown here.

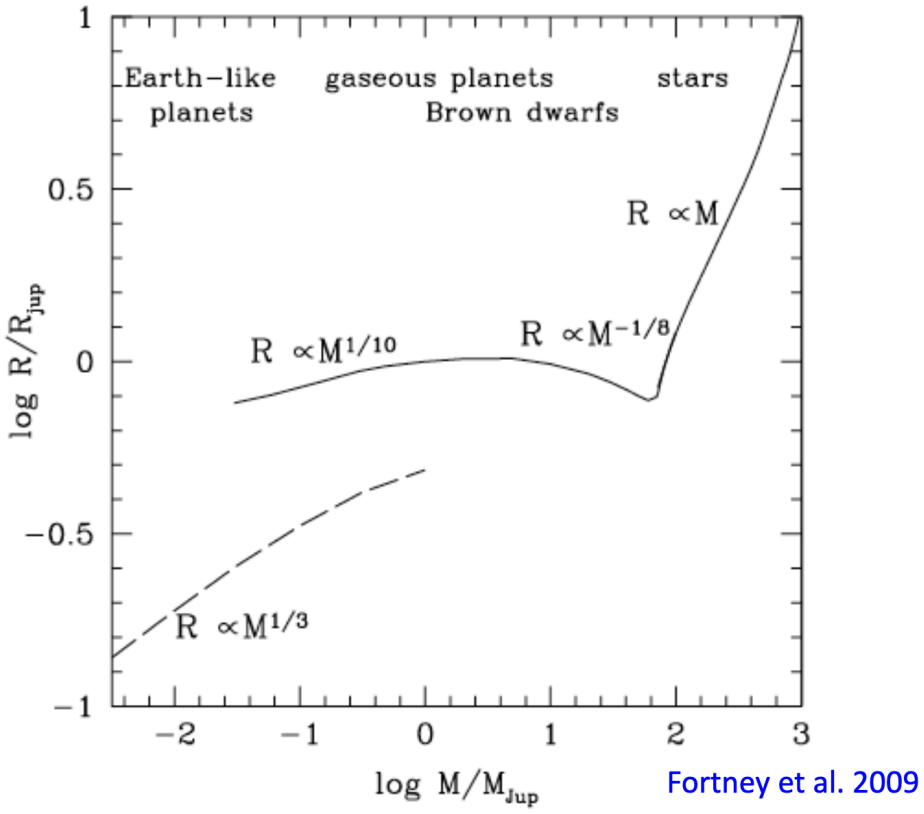

Fortney et al. 2009

Some qualitative interpretation of this plot: Neptune-like planets are below -1, stars are above 2, and the middle region is the gas giants up to brown dwarfs, and the nominal boundary between those is 13 M_J. We can see that in the absence of any additional source of energy, the plot peaks around $R = R_J$ and at $M =\sim M_J$ (where $\sim$ can be 1-5 because we're astrophysicists); Jupiter is about the biggest you can make a hydrogen-rich sphere.

What drives the transition from gas giant to brown dwarf? $13M_J$ is about where deuterium burning becomes significant; it's the point at which 50% of deuterium burns over a 10 Gyr lifetime of an object. This isn't an exact number, and anywhere from 11-16 may be good.

Even if you have deuterium burning, it may not be a significant source of energy in the smaller brown dwarfs. Further into the brown dwarf regime, you go from partial to complete degeneracy. For masses beyond the complete degeneracy cutoff at about 80 M_J, hydrogen burning starts and we go from brown dwarfs to stars.

It's notable that Jupiter and Saturn used to be our only datapoints for these relations, and now we've populated it with thousands of exoplanets and brown dwarfs.

Historically, people used zero-temperature equations of state $\rho = \rho(P)$ to generate theoretical mass-radius relations for cold spheres. They found a normal-ish distribution peaking and subsequently declining at around 0.1 M_J. With more and more data, we found a lot of planets around the mass of Jupiter, but with a much larger radius, which seems to contradict the peak around Jupiter that we saw before. What makes these exoplanets so much larger than the theoretical curves for H-rich spheres would suggest, when their composition isn't that different?

The answer is that these are hot Jupiters; they're highly irradiated and some of that energy gets deposited onto the interior and puffs up the radius. To analyze this in detail, we'll look at thermal evolution and luminosity evolution.

The initial stages of evolution involve gravitational contraction, and the fraction of the gravitational potential energy that goes into the planet's internal energy is governed by the virial theorem. We'll use the form $xE_i + E_g = 0$, where x is a fraction governed by material properties. This gives us $E_i = -\frac{1}{x}E_g$. The remaining energy $E_r = |-E_g| - E_i = -\frac{x-1}{x}E_g$ is radiated away; some constant fraction (which we can consider to be an efficiency factor η) of the gravitational energy contributes to the luminosity, which is governed by $L = \dot{E}_r$.

We know gravitational potential energy is given by $E_g = -\underbrace{\frac{3}{5}}_{\alpha}\frac{GM^2}{R}$, so following the above reasoning gives us

$$L = -\eta\frac{\mathrm{d}E_g}{\mathrm{d}t} = \frac{-\eta\alpha GM^2}{R^2}\dot{R} \tag{20.1}$$

or conversely, the contraction is governed by the luminosity,

$$\dot{R} = \frac{-LR^2}{\eta\alpha GM^2}. \tag{20.2}$$

At some point, this stops working as we start hitting degeneracy pressure. When the object has sufficient interior degeneracy, gravitational contraction is no longer the dominant source of luminosity because there isn't much more contraction that's possible. At this point, luminosity starts coming from the cooling of the ions in the interior, $L \sim -\dot{E}_{\text{ion}} \propto -\dot{T}_{\text{ion}}$. Giant planets start out large, luminous, and hot, and evolve into smaller, cooler, and less luminous objects.

Extrasolar Planets **Lent 2022**

Lecture 21: Interiors of giant planets

Lecturer: Nikku Madhusudhan *9 March* *Aditya Sengupta*

For qualitative purposes, we write $E_r \sim \eta\alpha\frac{GM^2}{R}$ to represent the amount of radiative energy available (taking the positive value to represent a sort of "energy budget") and we let η be a variable over time. In the early stages of evolution, we have $\eta = \frac{1}{2}$ by the virial theorem. For molecular hydrogen, it might be $\eta = \frac{2}{3}$, but it eventually gets much smaller. For Jupiter in the present day, $\eta \sim 0.03$.

Start with the usual luminosity relation, $L = 4\pi R^2\sigma T_{\text{eff}}^4$. As a planet evolves, it cools down, so T_{eff} goes down, and it contracts, so R goes down. Both of these contribute to L going down over time.

We can find a scaling relation for the cooling time:

$$\tau = \frac{E_r}{L} = \frac{\eta\alpha GM^2}{RL} \tag{21.1}$$

and conversely

$$L = \frac{\eta\alpha GM^2}{R\tau}. \tag{21.2}$$

That is, the luminosity of an object goes down over time, and a $\log L$ vs $\log \tau$ plot is a straight line representing a powerlaw.

Because R is contracting and then settling to its eventual radius, the plot of R over time has a fast dropoff for the first ~ 100 Myr, and reaches a relative steady state after that. The temperature decreases more monotonically than the radius.

Let's look at Jupiter as a test case. We saw it has $\eta \sim 0.03$ and $|E_g| = \frac{3}{5}\frac{GM^2}{R} \sim 2 \times 10^{43}$ erg. We have $E_r = \eta|E_g| \sim 6 \times 10^{41}$ erg. We also know that $L_{J,int} \sim 3 \times 10^{24}$ erg/s, which gives us a timescale $\tau \sim 6$ Gyr, longer than the current age of the solar system. We could also use this logic to estimate the current radius contraction $\dot{R}$ of Jupiter.

$$\dot{R} = -\frac{LR^2}{\eta\alpha GM^2} \tag{21.3}$$

There are two ramifications of this. The first is it's easier to see younger planets, because they're inherently more luminous. This helps us in directly imaging planets. The second is that the starting luminosity depends on the starting mass and energy, which in turn depends on the formation mechanisms which determine the initial entropy.

$$\frac{\mathrm{d}L}{\mathrm{d}r} = 4\pi r^2\rho\dot{\epsilon} \tag{21.4}$$

and we sometimes write $\dot{\epsilon} = -T\frac{\mathrm{d}S}{\mathrm{d}T}$, so we have a direct relationship to the entropy S. Short-timescale formation processes like gravitational instabilities tend to have higher entropy, and long-timescale formation like core accretion has lower entropy.

We can look at mass level curves of luminosity evolution over time. There's three general categories: stars, which lose some luminosity until hydrogen burning kicks in; brown dwarfs, which have a relatively gentle slope due to contributions from deuterium burning; and planets, which drop off the fastest.

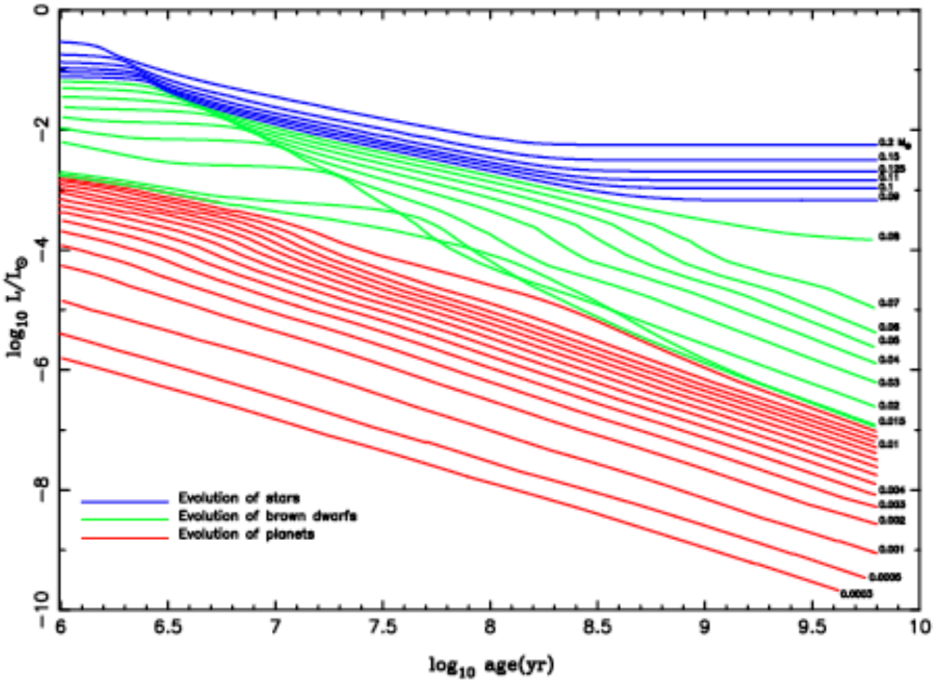

We still haven't resolved the inflated hot Jupiter issue, where hot Jupiters are much larger than Jupiter. There are two classes of explanation. The first is an external source of heating: this can be due to tidal dissipation of orbital eccentricity (energy due to circularization of an orbit; this can't be a universal explanation, as circularization timescales are relatively short so the planet would contract after it's over), atmospheric dynamics (recirculation of winds in the atmosphere), or ohmic dissipation (hot atmospheres can thermally ionize some of its constituents, forming currents that may enter the convective layer and dissipate power). Studies show we need about 1% of the incident radiation to be deposited in the interior of the planet. The second is stalling the contraction of the object, or reinflation after contraction. This can happen due to enhanced opacity, making cooling less efficient, or due to chemical gradients in the lower atmosphere causing convection and slowing the dissipation of energy outwards.

Finally, what are the interior compositions of these objects? We've been assuming that giant planets are mostly molecular hydrogen, which is true in the exterior. Going deeper, temperature and pressure increase and so hydrogen is thermally dissociated and ionized, so we have ionized hydrogen. Up until 2015, it was assumed there was a rocky core interior to this, but a more recent understanding (Miguel et al., 2022) suggests the core is more diffuse and less well-defined, and the interior is more characterised by a metallic gradient than an actual separate core.

Extrasolar Planets **Lent 2022**

Lecture 22: Interiors of rocky planets

Lecturer: Nikku Madhusudhan *11 March* *Aditya Sengupta*

While the interiors of gas giants are relatively dilute (based on *Juno* studies of Jupiter), showing a gradual gradient outwards from a core to a hydrogen envelope, ice giants and terrestrial planets have sharper boundaries. Ice giants like Uranus and Neptune may have up to 80-90% of their interiors made of ices and rock, and may have H/He envelopes up to 2 Earth masses; we don't have good enough measurements to constrain these for sure. The key difference we know is that ice giants are not hydrogen-rich in the interior, and we have much higher ($\sim$30x Jupiter's) metallicity. Meanwhile, terrestrial planets have complex structures: just looking at Earth, there's distinct regions in the core, mantle, and crust, which we know from seismology but don't necessarily know for terrestrial exoplanets. The compositions of rocky planets tend to be a lot more complex for these reasons. We don't know the mass fractions of these components upfront.

There's four dominant elements of the chemical compositions of the solar system planets:

1. iron/nickel (usually in the cores)
2. silicates (rock)
3. molecular hydrogen
4. water

The compositions of exoplanets may be significantly different, though. When we got the first datasets from *Kepler*, around 2010-2011, we noticed large populations of exoplanets between the boundaries of what we'd previously thought of as a classification system into terrestrial, icy, or gaseous planets; the most dominant planet type we know today is between the ice giants and Earth, dubbed *mini-Neptunes* and/or *super-Earths* (the exact boundary isn't clear). We should expect that compositions are just as diverse as the macroscopic properties.

We can start understanding the composition in terms of the structure equations. Rocky planets won't have much energy from gravitational contraction, but they may have other sources of $\dot{\epsilon}$ like radioactive processes.

Let $\rho = \rho_c$, a constant, and solve the structure equations (hydrostatic equilibrium and mass continuity) while imposing $P(R) = 0$ to get

$$P(r) = \frac{2\pi G}{3}\rho_c^2(R^2 - r^2). \tag{22.1}$$

If we plug in accepted values for Earth (take $\rho_c = 5.5\text{g/cm}^3$) we get $P_c \sim 150$ GPa. The actual value is about 350 GPa, which isn't bad as an astronomer's estimate but shows the effect of the density gradient is significant. This is the case because even for a one-material interior, the density won't be uniform with pressure. We usually have constant density until some critical pressure, and subsequent nonlinear (power-law) increase at high pressures. This translates to a bulk mass-radius relation. If we didn't have this compression effect, we'd expect that planets with radius $2R_E$ have mass $8M_E$, but there's significant deviations from this in the observed population; $8M_E$ planets have radii more like $1.5R_E$. There are standard forms for the equations of state for various types of planets. With additional volatile layers, the other structure equations become significant too.

We analyze this in practice (to zeroth order) by drawing level curves of the dominant elements and mixtures of them on $M - R$ diagrams, scattering the known planets, and noting which curves pass close to the points. The mass fractions are considered to be free parameters which we can iterate over; if we're taking three components, we vary two mass fractions and let the third be set based on the requirement that they sum to 1, note the resulting mass and radius, and see how closely it matches the observed mass and radius. These solutions are represented in what's known as a *ternary diagram*, which allow us to represent points in $\alpha + \beta + \gamma = 1$ space in terms of an equilateral triangle, and we can color regions of the triangle based on the calculation outcomes.

Case studies in this sort of compositional exploration is the super-Earth CoRoT 7b (silicate-rich, but with a wide range of other possible compositions if the uncertainties were increased 3x) and the mini-Neptune GJ 1214b (ice+rock interior with a hydrogen envelope, or a water world with a steamy atmosphere; the possible hydrogen envelope composition is very well constrained at $< 10\%$).

The solar composition can be significant too. The super-Earth 55 Cancri e is at about 2400K and is above the silicate curve, so some sort of water-rich or hydrogen-rich envelope is necessary but is difficult to sustain; volatile layers would dissociate very fast. The usual oxygen-rich models need a layer of super-critical water to resolve this. However, if we took a solar composition (assuming the protoplanetary disk matches the stellar abundances), the star's greater C/O ratio would enable us to consider other molecules, like silicon carbide, that may dominate the composition. In this case, the M-R curves for carbon and silicon carbide ended up going right through the point for 55 Cancri e.

The other thing that matters is atmospheric observations. When we're considering the radius of a rocky planet, we usually just want R_p, but we can observe $R_p + H$. In the early stages of observing rocky planets, this was neglected, because we didn't have the sensitivity that would make that significant, but now, it does make a difference. Looking at transmission spectra in their gaps, where possible, can give us a more accurate R_p (but generally it's better to couple this to a full atmospheric model). There are numerous ongoing missions, like TESS and CHEOPS, that aim to constrain these observables even more precisely. We can also note that the equilibrium temperatures of rocky planets can be greater than the melting temperatures of the rocks. This rules out effects we're used to on Earth, like separate land and water regions and plate tectonics, and at a certain point the surface would be mostly molten, giving rise to magma ocean worlds.

Extrasolar Planets **Lent 2022**

Lecture 23: Habitability

Lecturer: Nikku Madhusudhan *14 March* *Aditya Sengupta*

Annoyed at myself for deleting this by accident.

Extrasolar Planets **Lent 2022**

Lecture 24: The search for biosignatures

Lecturer: Nikku Madhusudhan *16 March* *Aditya Sengupta*

Annoyed at myself for deleting this by accident.